This is to certify that the
dissertation entitled

PERFORMANCE STUDY OF A REGENERATIVE FLOW
COMPRESSOR AS A SECONDARY AIR PUMP FOR
ENGINE EMISSION CONTROL

presented by

YOUNES ELKACIMI

has been accepted towards fulfillment
of the requirements for the

Ph.D. degree in Mechanical Engineering

Major Professor's Signature

June 29, 2007

Date

PERFORMANCE STUDY OF A REGENERATIVE FLOW COMPRESSOR AS A SECONDARY AIR PUMP FOR ENGINE EMISSION CONTROL

By

Younes Elkacimi

A DISSERTATION

Submitted to
Michigan State University
in partial fulfillment of the requirements
for the degree of

DOCTOR OF PHILOSOPHY

Department of Mechanical Engineering

2007

ABSTRACT

PERFORMANCE STUDY OF A REGENERATIVE FLOW COMPRESSOR AS A SECONDARY AIR PUMP FOR ENGINE EMISSION CONTROL

By

Younes Elkacimi

This thesis reviews the status of regenerative flow pumps and compressors (RFP/RFC) for fuel emission reduction, and proposes design guidelines with the aim to improve their flow and efficiency. A brief overview of the fundamentals and hypothesis of the operation of RFP/RFC is presented. An analytical model for regenerative flow pumps and compressors is developed, and a one-dimensional (1-D) performance prediction code of an RFP/RFC model is synthesized using geometric parameters as input. Based on these predictions, design guidelines to improve performance of these turbomachines are proposed. CFD analysis is undertaken to validate these proposed design changes. Prototypes of current and proposed design changes of regenerative flow pumps and compressors are built and tested, and experimental data is studied and compared to the theoretical and numerical simulation findings. Sensitivity analysis is conducted on various design parameters to study their effect on the device's performance, and designs for optimum performance were created. The design approach is generalized and applied to a larger family of RFP pumps and compressors. A streamlined approach to RFC/RFP improvement is developed for future applications and more efficient regenerative flow pumps, which are the result of this study, are built, tested, and used in current applications for emission reduction and control in passenger and industrial vehicles.

To my parents' vision, sacrifices, and complete belief in me

ACKNOWLEDGEMENTS

First, I would like to thank Allah for giving me the strength and the ability to reach this point in my academic career. My parents have been a great source of encouragement and support throughout my life, and I want to take this opportunity to thank them from the bottom of my heart for all they have done for me. I, especially, am fond of my father, may Allah bless his soul, for his care and genuine support of all my ambitions and goals. My dear mother has continued to be very supportive of my career long after my father's passing. I'm very grateful to her for all her sacrifice. This thesis could not have seen the light of day without the great and fundamental support of my professor, mentor, and main advisor Dr. Abraham Engeda. I am especially thankful to Dr. Engeda for his original ideas, creative problem-solving methods, and continuous support of this research since its inception. I have learned so much from him not only in the fields of turbomachinery and thermodynamics, but also about life in general. I would also like to thank all of my committee members, Dr. Norbert Muller, Dr. Craig Somerton, Dr. Chia Chiu, and Dr. Hassan Khalil for supporting this research and guiding me through it, and for all the assistance they have offered me. Dr. Clarck Radcliffe has been very influential in getting this research done and I am very indebted to him for all his efforts and tremendous support. I would like to thank Mr. Kevin Liske, Mr. Ketan Adhvaryu, and Mr. David Kaitschuck from BorgWarner for all their help and advice in completing this work. They have been very supportive of this research, and have offered an incredible amount of assistance and technical guidance to facilitate this work and make it a success. BorgWarner and its people have been very instrumental in this research and put in a lot of effort, generated a great deal of interest, and provided a lot of support to get this work completed, help further this research endeavor, and create new knowledge in this very promising field of turbomachinery. I am thankful to my colleagues from the mechanical engineering department, namely Mr. Omar Farooq, Dr. Muhammad Mukarrum Raheel, Dr. Elliot Motato, as well as others for their advice, technical help, and very productive discussions we have had throughout my graduate studies at MSU. I want to, also, very much thank Ms. Aida Montalvo at the ME department, who has been of tremendous support to me over the years. She has facilitated many tasks for me and helped me a great deal with a lot of administrative and other work. She is without a doubt one of the best and most helpful people I have come to know at MSU. Last, but not least, I would like to thank anybody whose name I have not mentioned, who has supported me with this research one way or other, directly or indirectly, from Michigan State University or elsewhere.

TABLE OF CONTENTS

LIST OF FIGURES

NOMENCLATURE

Notation

A	cross sectional area
AR	channel aspect ratio
c	tip gap
a_c	shear area of casing
a_i	shear area of impeller
A_b	area of blade
A_c	channel area
A_R	area at any radial location R_p
b	blade depth
BF	blade blockage factor
c_a	axial clearance
c_r	radial clearance
C_D	orifice coefficient
h	blade height
H	head
K	blade aspect ratio
Q	volumetric flow rate
Q_s	solid body rotational flow rate in channel
Q_v	solid body rotational flow rate in vane

Q_c	circulatory flow rate
Q_{leak}	leakage flow rate
$\dot{Q}$	heat transfer rate
r	radial distance to centroid
r_o	radial distance to impeller hub
r_2	radial distance to impeller tip
r_3	radial distance to channel tip
R	radius of curvature
t	blade thickness
Z	number of impeller blades
ϕ	non-dimensional flow coefficient
δ	stripper clearance
σ	slip-factor
ω	angular speed
α	incidence factor
β_{in}	blade inlet angle
β_{ex}	blade exit angle
ψ	non-dimensional head coefficient
$\Delta\psi$	non-dimensional head loss
C_c	shear stress coefficient of casing
C_D	orifice discharge coefficient
C_i	shear stress coefficient of impeller

C_p	specific heat at constant pressure
d_A, d_B	channel depth at station A and B
dX_G	peripheral distance
D_h	hydraulic diameter
e	impeller blade height
f_R, f_C	rotor and casing friction factor
F_s	fraction of periphery occupied by impeller seal
g	acceleration due to gravity
H_b	aerofoil blade height
H_1, H_2	total enthalpy of fluid at inlet and exit of impeller blade
K_b	blade turning loss coefficient
K_{in}, K_{out}	inlet and discharge port loss coefficients
K_s	blade mixing loss
K_{se}	sudden expansion loss
k_t	channel turning loss coefficient
K_t	head loss coefficient
l	aerofoil blade chord length or Flow path length
L_1, L_2	length of blading at inlet and outlet edges
$\dot{m}$	mass flow rate
$\dot{M}_A$	mass flow rate through annular channel

$\dot{M}_B$	mass flow rate through blading
N_B	number of passages of fluid between inlet and outlet ports
N_s	specific speed
p	pressure
p_{in}, p_{out}	inlet and discharge pressure
$\dot{P}_{decomp.}$	decompression power
$\dot{P}_{disk}$	disk friction loss power
$\dot{P}_{hyd}$	hydraulic power
$\dot{P}$, P	power
PC	pitch to cord ratio
$\dot{q}$	non-dimensional heat transfer rate
r_G	centroidal radius
R	gas constant
Re	reynolds number
S	transverse component of path length
T	torque, Temperature
T_1, T_2	absolute temperature of fluid at inlet and exit port
U_1, U_2	tangential velocity of impeller at hub and tip
V_c	circulatory velocity
V_θ	tangential velocity
V_m	mean tangential fluid velocity

$V_{\theta 1}, V_{\theta 2}$	tangential velocity of fluid at inlet and exit of impeller
W_1, W_2	relative velocities of fluid with respect to blading
Z_s	number of blades in stripper

Symbols

α	shock loss coefficient
β	blade angle
β_1, β_2	fluid angles at inlet and outlet edges of blading
γ	ratio of specific heats
Υ	power coefficient
η	efficiency
ρ_1, ρ_2	density at inlet and outlet edges of blading
ρ_M	mean density of fluid in annular channel
ω	RPM
θ_p, θ_s	pumping and stripper angle respectively
σ	slip factor
Ψ	head coefficient
λ	flow coefficient
Π	pressure ratio
Φ	specific mass flow rate

Subscripts

c	circulatory flow
des	design point
l	leakage
o	open channel
θ	peripheral direction
st	stripper region
v	vane

CHAPTER 1

INTRODUCTION

1.1 Turbomachinery

Turbomachines are devices associated with fluid circulation. They either extract or add energy to fluids by the dynamic action of one or more moving parts. Such machines as pumps, compressors, fans, and turbines are classed as turbomachines [1]. Turbomachines constitute a large class of machines, which are found virtually everywhere and are used in ever increasing applications. Turbomachines can be of different types, such as turbines, compressors, and pumps, depending on their application.

Turbomachines are composed of certain essential elements, the most important of which is the rotor, and the fluid circulation in these machines always involves an energy transfer between a flowing fluid and a rotor. The latter changes the kinetic energy, stagnation pressure and enthalpy of the fluid.

As a member of the turbomachine family, pumps are a generic classification that includes any turbomachine, which transfers energy from rotor to fluid, such as blowers and fans, with the main purpose being to pressurize fluid. Turbines, on the other hand, are machines, which transfer energy from the fluid to the rotor and are mainly used for energy production. Pumps are also classified based on their operating concept, and they are specifically, positive displacement and dynamic (momentum change) pumps.

The compressor rotor may be thought of as an air pump. There are various types of compressors, which span a large range of service requirements as shown in Figure (1). Generally speaking there are two basic compressor types: continuous flow compressors and positive displacement compressors. Continuous flow compressors accelerate the fluid to a high velocity and then translate this kinetic energy into potential energy. Centrifugal, axial, mixed type, and regenerative compressors are all continuous flow compressors.

Positive displacement type compressors are available in two types: rotary and reciprocating compressors. In rotary compressors, male and female screw-rotors mesh, trapping air and reducing the volume of the air along the rotors to the air discharge point. Reciprocating compressor operates a piston reducing the volume in the cylinder occupied by the gas and then compresses it to a higher pressure. In the positive displacement type, a given quantity of gas is locked in a compression chamber and the volume, which it occupies, is mechanically reduced. At constant speed, the airflow remains constant with variations in discharge pressure.

Positive displacement pumps and compressors deliver moderate flow rates and produce high-pressure rise. They deliver pulsating or periodic flow and have small range of flow rate operation. Dynamic pumps and compressors, on the other hand, have a larger range of flow operation and typically deliver higher flow rates and produce high-pressure rise. They are very sensitive to fluid viscosity as opposed to their positive displacement counterparts.

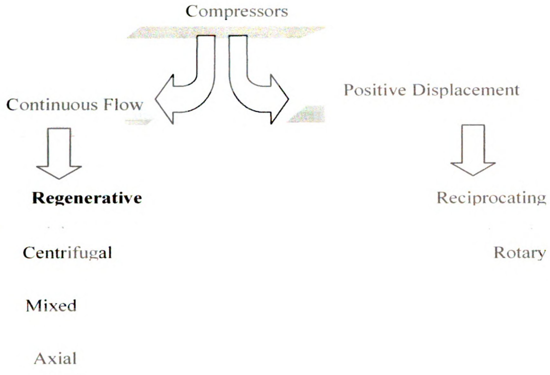

Figure 1: Categorization of Compressors

Sizes of turbomachines vary widely from hundreds of microns to several meters in diameter, and their fluid states vary broadly as well. The materials encountered in these machines are usually selected to fit the temperature, pressure, and chemical nature of the fluids handled and the manufacturing methods used.

The most popular pumps and compressors are the centrifugal, regenerative, axial and radial.

1.2. Centrifugal Air Pumps and Compressors

One way of classifying centrifugal pumps is based on the way in which fluid flows through the pump. The behavior of fluid flow through the pump is determined by the design of the pump casing and the impeller. Centrifugal pumps basically consist of an impeller mounted on a rotating shaft and a stationary pump casing. The pump casing provides a pressure boundary for the pump and contains channels, which act as guides to direct the suction and discharge flow. The pump casing has an inlet and an outlet for the main flow path of the pump. Figure (2) is a cutaway schematic of a typical centrifugal pump that shows the relative locations of the pump suction (point 1), impeller, volute, and discharge (point 2). Figures (4 and 5) show impeller X, which is a five-bladed centrifugal pump impeller, and the volute A designated to match it and was often tested with it. The pump casing guides the liquid from the suction connection to the center, or eye, of the impeller. The liquid is imparted to the outer periphery of the pump casing by the vanes of the rotating impeller. Then, it is collected in the outer part of the pump casing called the volute. The volute, which has the purpose of collecting the liquid discharged from the periphery of the impeller at high velocity and gradually causing a reduction in fluid velocity by increasing the flow area, expands in cross-sectional area as it wraps around the pump casing. This kinetic energy created by the centrifugal force in this process is transformed into static pressure.

The amount of energy given to the fluid is proportional to the velocity at the edge or vane tip of the impeller. The kinetic energy of the fluid displaced by an impeller is harnessed by creating a resistance to the flow. The pump volute (casing) that catches the liquid and slows it down creates this resistance. The bigger the impeller is, or the faster it revolves, the higher the velocity of the liquid at the vane tip will be, and in turn the greater the energy imparted to the liquid. In the discharge nozzle, the liquid further decelerates and its velocity is converted to pressure according to Bernoulli's principle.

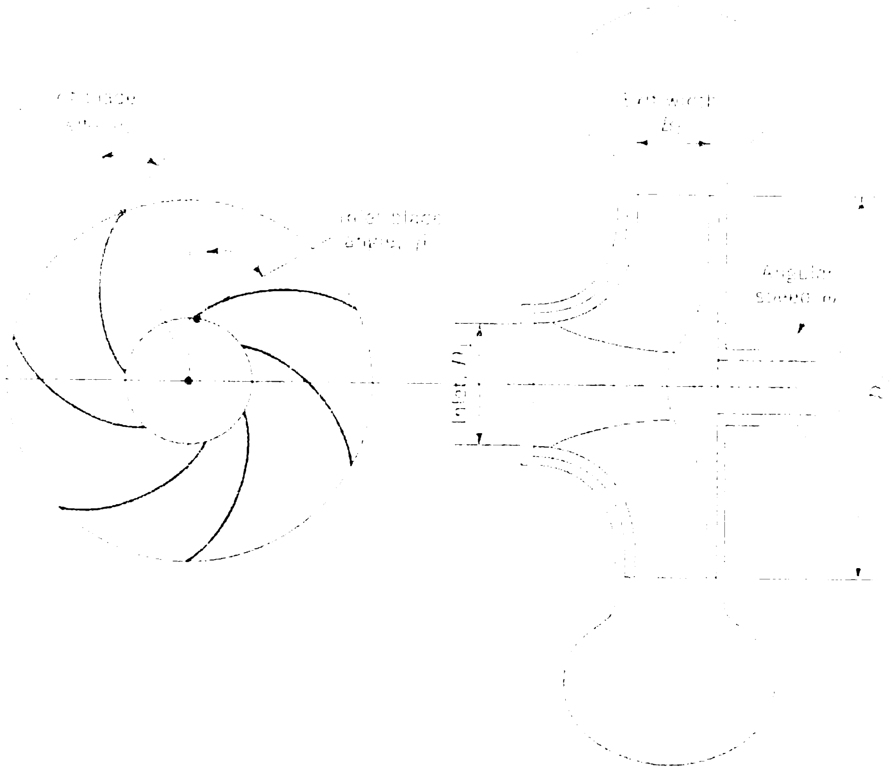

Figure 2: Cutaway schematic of a typical centrifugal pump

The three types of flow through a centrifugal pump are axial flow, radial flow, and mixed flow.

Axial flow pumps, which are also called propeller pumps, have an impeller, which pushes the liquid in a direction parallel to the pump shaft. Two particular axial flow pumps or inducers are shown in Figure (3). Axial flow compressors have the advantage of being capable of very high compression ratios with relatively high efficiencies. Axial compressors, which are made of a stationary set of airfoils called stator vanes and a series of rotating airfoils called rotor blades, typically utilize multiple stages and produce higher-pressure rise per stage. The entire compressor is made up of a series of alternating rotor and stator vane stages as shown in Figure (6). A stage consists of two rows of blades, one rotating and one stationary. The air is compressed in a direction parallel to the axis of the engine.

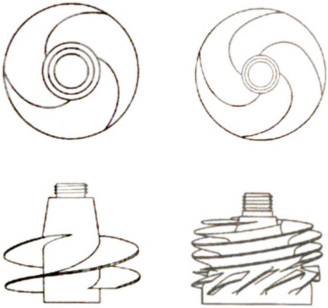

Figure 3: Pump inlet inducer (after Brennen [6])

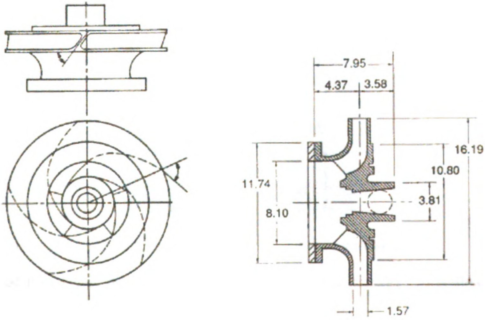

Figure 4: A centrifugal pump impeller designated Impeller X (after Brennen [6])

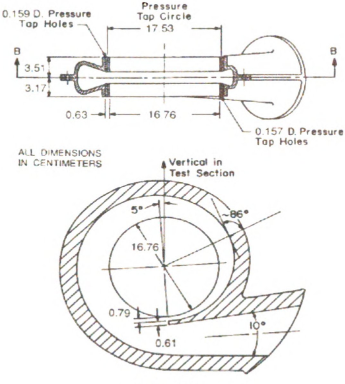

Figure 5: A vaneless spiral volute (designated Volute A) designed to be matched to Impeller X (after Brennen [6])

Figure 6: An axial compressor – (single rotor)

In a radial flow pump, the liquid enters at the center of the impeller and is directed out along the impeller blades in a direction at right angles to the pump shaft. The impeller of a typical radial flow pump and the flow through a radial flow pump are shown in Figure (7) below.

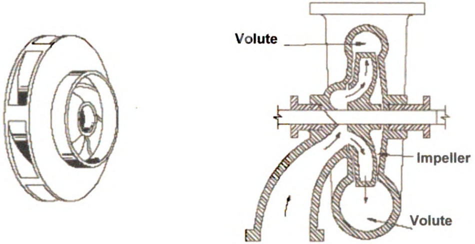

Figure 7: Radial Flow Centrifugal Pump (after [32])

Mixed flow centrifugal pumps combine impeller blade features from both the axial and radial flow pumps. The impeller blades push the fluid out away from the pump shaft and to the pump discharge, as the fluid flows through the impeller of a mixed flow pump. The flow through a mixed flow pump and the impeller of a mixed flow pump are shown in Figure [8].

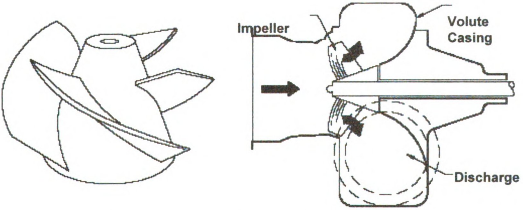

Figure 8: Centrifugal Mixed-flow Pump (after [32])

1.3. Introduction to Regenerative Flow compressors and Pumps

Regenerative flow compressors and pumps (RFC/RFP) are rotordynamic machines capable of producing high heads at very low flow rates. With a single rotor, RFP/RFC machines can deliver heads comparable to that of several centrifugal stages. Regenerative flow pumps have very low specific speed and share some of the characteristics of positive displacement machines. In literature, the regenerative flow pumps are also known as peripheral pump, drag pump, traction pump, Tangential pump, side-channel pump, and Vortex pump.

There is a body of knowledge on the subject of turbomchines in general, although the literature on regenerative flow pumps and compressors in particular is not extensive. This knowledge combines mathematical analysis, fluid mechanics and thermodynamics, computational fluid dynamics, and other important scientific ingredients. Secondary air pumps, however, have not been given much consideration over the years considering they have been used for decades in many applications, which are constantly increasing. The efficiency of RFP pumps is relatively low compared to that of centrifugal pumps, usually less than 40%, but they still find many applications in the industry. Applications in emissions reduction in automobiles, aerospace and automobile fuel pumping, agricultural industries, chemical and foodstuffs industries, water supply, and shipping and mining to name a few.

Figure (9) shows a picture of a RFP for air delivery to an auto exhaust system delivery for emission reduction applications.

Figure 9: Electric Air Pump (Courtesy BorgWarner)

1.4. Applications of RFP/RFC

The efficiency of RFP/RFC is not as high as that of centrifugal pumps and compressors, and is usually less than 50%. Some of the best and most efficient RFP pumps and compressors have efficiency in the low to mid 40%. However, regenerative flow compressors and pumps are more compact and have other advantages, which make them very viable for many applications, especially the ones that require high delivery head at low flow rates. The regenerative gas compressors and liquid pumps have important applications as gas circulators and liquid pumps in accessory systems. They have found many applications in industry because they allow the use of rotor-dynamic action in place of positive displacement actions. RFP/RFC pumps and compressors are being used in increasing number of applications, because of their relative simplicity of construction and stable operating, and making them more and more attractive to users in several areas, including automotive, nuclear, chemical, and petroleum industries. Other applications of RFC include phase reactor recycling, vent/purge gas recovery, boosting and recycling of hydrogen mixtures and hydrocarbon gases, and gas compression in many industrial processes.

RFCs, for instance, have been used as natural gas and hydrogen pipeline compressors. A four stage regenerative compressor, which was employed in the development of a highly reliable, long life cryogenic refrigerator for space vehicle application Gessner reports. One of the recent applications of regenerative flow compressors is in accessory loops and auxiliary systems for nuclear pile operation, thanks to their ability to be incorporated in small closed cycle helium refrigerators. In addition to their compact size, low maintenance, and reliability, recently there is an increasing use of regenerative compressors in low-pressure (0.2 - 15 psig) microturbine systems for natural gas compression.

Regenerative flow compressors are very competitive with other turbomachines especially at relatively low specific speeds (Figures (10 and 11)) below. Better efficiency at low specific speeds makes regenerative flow pumps and compressors strong competitors to centrifugal turbomachines in low specific speed applications. This is why the industry is interested in conducting more research and making design changes in RFC/RFP to improve their performance and make them more attractive to industry in different applications.

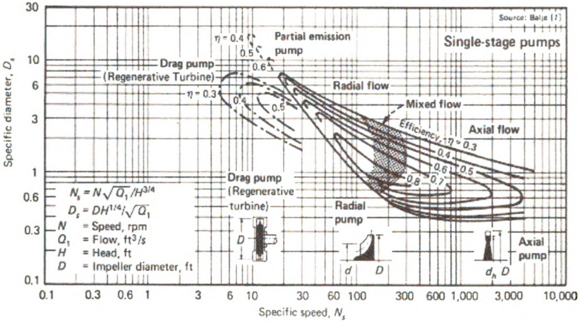

Figure 10: Ranges of specific speeds for typical turbomachines and typical pump geometries for different design speeds

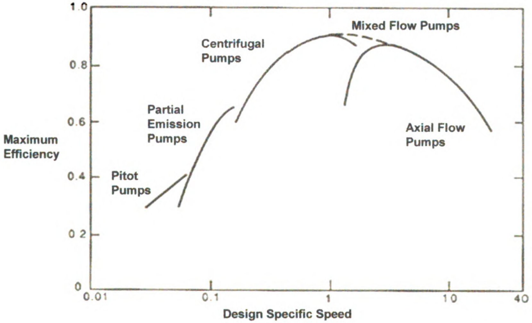

Figure 11: Maximum efficiency vs. Design specific speed for different pumps (after [6])

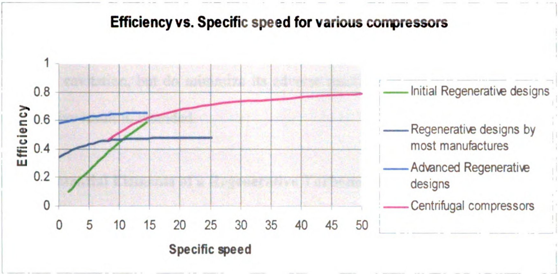

Figure 12: Efficiency vs. specific speed for various compressors

$SpecificSpeed = N = \frac{\omega\sqrt{Q}}{H^{\frac{3}{4}}}$, where Q is the flow rate, w the rotational speed, and H the head.

One of the advantages of regenerative pump, which makes it applicable in many industries, is that its operation under cavitation does not generally lead to mechanical failure. It has been established that cavitation refers to the formation of vapor bubbles in regions of low pressure within the flow field of a liquid [6]. Cavitation has adverse effects on the pump performance. Cavitation can cause damage to the material surfaces close to the area where the bubbles collapse when they are convected into regions of higher pressure. Cavitation damage can be very expensive, and very difficult to eliminate. For most designers of hydraulic machinery, it is the preeminent problem associated with cavitation. Another adverse effect of cavitation is that the performance of the pump, or other hydraulic device, may be significantly degraded. A third adverse effect of cavitation is less well known, and is a consequence of the fact that cavitation affects not only the steady state fluid flow, but also the unsteady or dynamic response of the flow.

This change in the dynamic performance leads to instabilities in the flow that do not occur in the absence of cavitation. Regenerative flow pumps and compressors might eliminate cavitation, but do minimize its adverse reactions in many applications, where that positive result in intended.

1.5. Essential Elements of a Regenerative Turbomachines

The essential elements of a regenerative turbomachine are shown in Figure (13), which illustrates a CAD design of the different components composing the T3 electric air pump of BorgWarner. The main components are the impeller, inlet port, discharge port, stripper, flow passage and a casing. Some of these components are discussed further in the next few paragraphs.

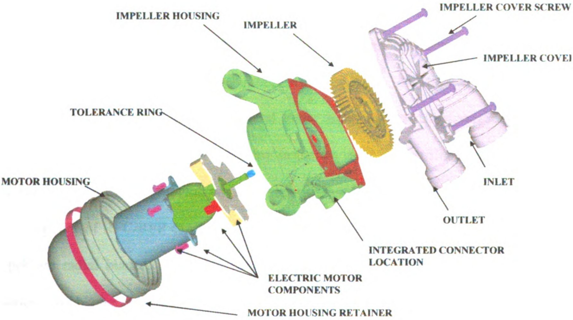

Figure 13: Electric Air Pump Components (Courtesy BorgWarner)

Impeller

Regenerative turbomachines employ a free-rotating impeller just like other types of continuous flow compressors and pumps. The impeller has vanes machined into either one side or both sides at its periphery, which due to their rotation produce a series of helical flow pattern, returning the fluid repeatedly through the vanes for additional energy as it passes through an open annular channel (torus). The fluid does not discharge freely from the tips of the blades but circulates back to blades many times before leaving the impeller, thus the term regenerative, which the name of the turbomachine implies. The helical flow motion has a gradual increase of air pressure in the tangential direction. This helical motion is created by the impeller vanes, which are stacked in series one after the other, instead of parallel to each other. This design configuration makes them different from centrifugal turbomachines.

Two types of fluid motion are combined to form the helical corkscrew motion describing the overall flow pattern of the regenerative turbomachine. The first one is made of a peripheral motion induced in the peripheral stator channel by the rotation of the impeller. The second motion is a circulatory motion in the rotor air passages and stator caused by the centrifugal pressure gradient, which is superimposed on the first motion.

The impeller of RFC/RFP can have blades of different shapes. Some of the widely used types are radial blades, non-radial blades Figure (14), semi-circular blades and airfoil blades. The blades or vanes are usually cast into the face of the impeller or machined at the periphery. The blades can be constructed as a single row, or as two rows side by side.

Flow Channel

The annular channel or torus has a cross-sectional area with a radius larger than that of the impeller vanes, and works as a wall boundary to the air flow once it exits circulates through the flow passages created by the successive impeller vanes. Flow channel cross-section and air passages are shown in Figures (15 and 16).

The fluid between the vanes is thrown out and across the annular channel. Turbulence, which causes loss of power and efficiency, is therefore generated as a result of the strong circulatory motion and mixing of the flow, which takes place as the flow hits the channel wall and recirculates back into the impeller air passages. The angular momentum acquired by the fluid in its passage between the vanes is transferred to the fluid in this annular channel.

Suction/Discharge/Stripper

The flow to the RFP is introduced to the impeller blades through the inlet (suction). The inlet controls how the fluid (air) gets in contact with the blades' surfaces, which in turn affects the flow behavior inside the air passages in the regenerative turbomachine, and sets up the spiral flow around the annular channel. The inlet for an axial SAP is shown in Figure (14). The outlet connects the flow to the external system piping and discharges it at high pressure into the system the fluid is targeting, which in the case of an emission reduction application, is the exhaust system of a gas or diesel operating vehicles.

The stripper is the part of the pump, which serves to block the high pressure at the discharge port from leaking to the suction port, and forces the fluid to exit out the outlet port. In addition to that, the stripper helps maintain the flow pattern of the fluid inside air passages in the torus. The stripper clearance between the impeller disk and the casing is kept to a minimum to prevent leakage from the high pressure side back to the low pressure side, and for secondary air pumps is usually in the order of tens of microns.

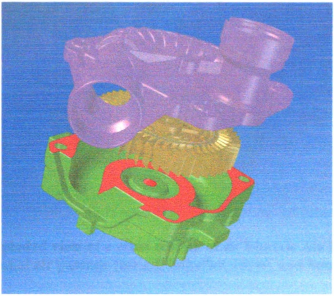

Figure 14: Electric Air Pump showing impeller, cover, and housing

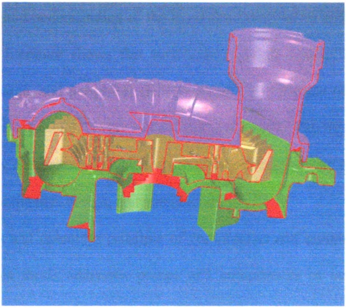

Figure 15: A cross sectional view of an Electric Air Pump showing channel air passage (torus), impeller, cover, and housing

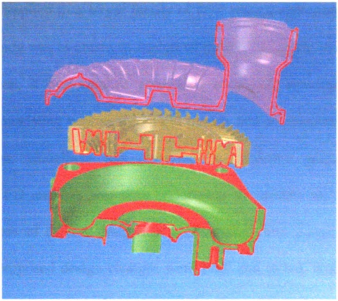

Figure 16: Exploded view of a cross section of an Electric Air Pump showing channel air passage (torus), impeller, cover, and housing

1.6. Objective of Research

It is strongly believed that a substantial amount of pressure and efficiency gains can be obtained from a good understanding of the exact flow mechanism and associated losses. Initial review of literature shows that such losses include hydraulic, shock, leakage, suction and discharge, and peripheral friction losses. The process of designing pumps and turbomachines in general, is very seldom straightforward. The final design is usually the result of many compromises, which involve several engineering disciplines such as fluid dynamics, mechanical design, and manufacturing.

The fundamentals and operating principle of compressors and pumps are very similar, which is why this thesis addresses pumps and compressors in tandem, particularly regenerative flow pumps and compressors. This thesis reviews the status of RFP/RFC, specifically, a secondary air pump model for fuel emission reduction, and proposes design guidelines with the aim to improve its flow and efficiency. The design approach is generalized and applied to a larger family of RFP pumps and compressors. The first objective of this study was to create an analytical model for regenerative flow pumps and compressors. Then, a performance prediction code was developed to predict the performance of the existing regenerative flow pumps and compressors. Based on these predictions, design guidelines are proposed to improve performance of these turbomachines. CFD analysis was then undertaken to validate these proposed design changes. Prototypes of current designs of regenerative flow pumps and compressors, along those with proposed design changes were built and tested, and experimental data collected, studied, and compared to the predicted results and numerical simulation findings. This research is conducted in collaboration with an industry leader and world supplier of secondary air pumps; their facilities were used to build and test the prototypes used in this research. Sensitivity analysis was conducted on various design parameters to study their effect on the device's performance. A systematic approach for the development and performance enhancement of RFC/RFP is developed in this thesis.

CHAPTER 2

GENERAL THEORY AND SIGNIFICANCE OF WORK

In order to find the combination of the pump/compressor design variables that maximizes the target value, an optimization algorithm is developed based on the desired application and the multiple design parameters involved. The objective here is to maximize the best efficiency value of the pump/compressor, using as design variables the pump/compressor input parameters.

2.1 General Theory

The automotive engine requires a relatively rich mixture of fuel and air for smooth operation on cold start. Exhaust gases contain high levels of carbon monoxide and hydrocarbons after cold starts. The unburned hydrocarbons could be further oxidized, except there is no oxygen left after combustion. By feeding air into the exhaust manifold (secondary air), CO and HC are oxidized through afterburning at temperatures over 600°C to form water and carbon dioxide. An activated secondary air injection system leads to an increase in oxygen content in the exhaust (air flow from the secondary air pump). This increase is noted by the Engine Control Unit, (ECU) (1) Figure (17) by reduced pre-cat (5) oxygen sensor voltage. The (ECU) operates in open loop mode with a fixed fuel map for the first 20 to 120 seconds of engine operation until the oxygen sensors have heated to operating temperature. To achieve efficient warm-up operation, a high secondary airflow rate must be achieved within the first few seconds of engine startup, and the airflow rate must be maintained until oxygen sensor control is in operation. Airflow is maintained by an electric air pump (6). Once the oxygen sensors and catalytic converters have reached their operating temperatures, valves (4, 7) cut off the secondary airflow.

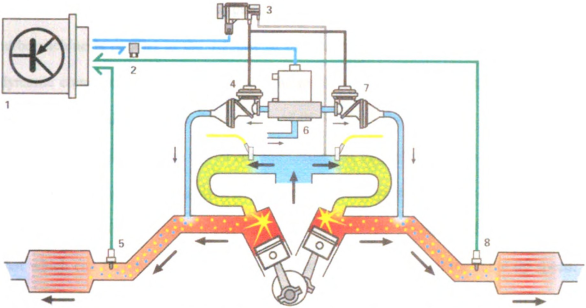

Figure 17: A schematic illustrating the secondary air pump within the exhaust system of an automobile

1. Engine Control Module (ECU)
2. Secondary air injection pump relay
3. Secondary air injection valve control, Bank 1 and 2
4. Multi valve, Bank 1
5. Oxygen sensor, pre-cat, Bank 1
6. Secondary air injection pump
7. Multi valve, Bank 2
8. Oxygen sensor, pre-cat, Bank 2

2.2 Working Principle

Two types of flow motion compose the helical flow pattern the fluid takes inside the regenerative flow compressors and pumps. The direction of flow through the RFC/RFP turbomachine is parallel to the velocity of the blades, as apposed to conventional fluid dynamic compressors and pumps, where the predominant direction of flow through the machine is at right angles to the velocity of the blades. Superimposed on the parallel flow is a circulation through the blades and around the core of the annular channel. The flow passes through the same blade row several times between the entry and the exit, and as a result, the work done on it and hence the pressure rise is considerably greater than that which can be obtained from a conventional turbomachine with the same tip speed. This is because every time the fluid passes through the rotor, work is done on it and its peripheral velocity and stagnation pressure are increased. The magnitude of the flow tangential velocity will be reduced by the action of tangential pressure gradient around the periphery of the machine between the exit conditions, and its direction will be reversed by the time the fluid re-enters the blade row. The pressure of the fluid changes as it flows through the regenerative pump as is illustrated in Figure (18).

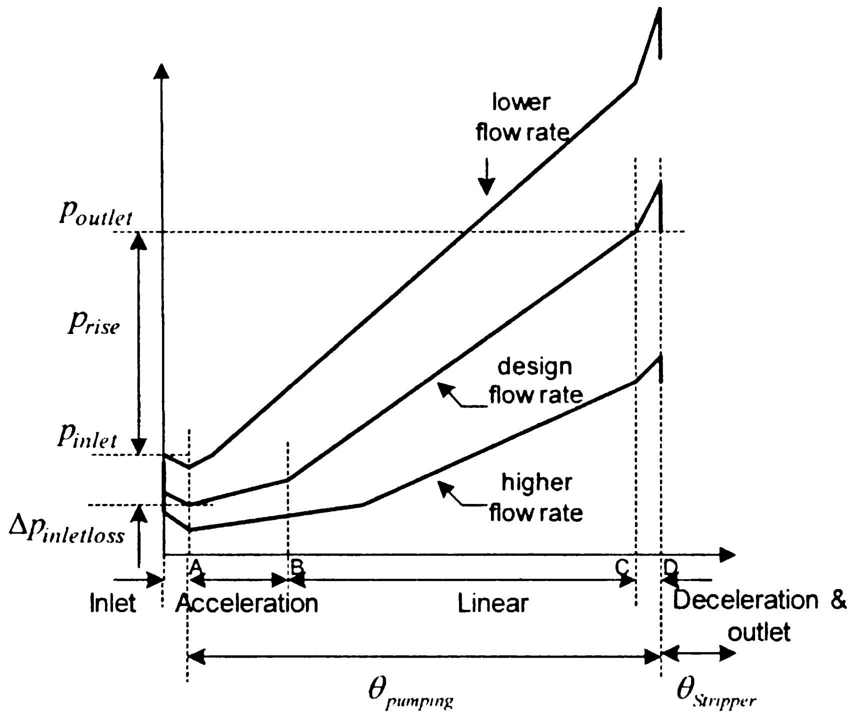

Figure 18: Tangential pressure deviation in a regenerative flow turbomachine

The flow experiences pressure loss as it enters the pump through the inlet region (A). This region has been proven experimentally to have a great effect on the flow pattern inside the pump, and in turn on the performance of the pump. The flow gets accelerated after that as it flows through region (A-B). The flow enters the working section of pump (region B-C) with a velocity and pressure dependent largely on the inlet region. This working region is linear, where the flow pattern becomes fully developed and the flow experiences a significant pressure rise. There is a little pressure rise in section (C-D), before the fluid exits the pump, where a deceleration of the flow occurs and the kinetic energy of the circulatory velocity is transformed into a pressure rise. The last step occurs when the fluid experiences a pressure loss similar to that at the inlet region, as it leaves the pump at the outlet (region D).

2.3 RFC/RFP vs. Centrifugal

Both regenerative flow and centrifugal flow compressors and pumps are employed in many applications in different industries today. Both of them have their own advantages and disadvantages. The regenerative flow compressors are more suitable for some applications while the centrifugal compressors are suitable for others.

One of the most significant structural advantages of the regenerative type compressors is that no complex flow passages or vanes are required. They are simple and easy to machine and do not use diffusers or scrolls. In regenerative compressors, the suction and discharge nozzles are at periphery, thus the axial and radial dimensions are small compared to centrifugal compressor, and thus provide much more pressure rise in a more compact compressor design. In regenerative flow compressors, fluid is exposed to impeller many times, thus adding more energy to the fluid as apposed to centrifugal compressors, where the fluid passes through the impeller only once. So, this explains why it takes a centrifugal compressor with many stages to produce the same head rise a regenerative compressor makes at the same tip speed. Regenerative flow compressors have head coefficients greater than 5 compared to about 0.7 to 0.8 for their centrifugal equivalents. One reason for that is because regenerative compressors impart both radial and an axial component to fluid flow, while centrifugal compressors take in the fluid at center of the impeller and push it radially outward with no axial component of velocity. Moreover, centrifugal compressors have large overall diameter because of diffusers and scrolls, and have a larger axial length per stage compared to their regenerative counterparts. Thus centrifugal compressors need higher rotating speeds or a large number of stages to offset and match the head rise difference between them and regenerative compressors.

The geometrical design of both types of compressors affects their performance. The regenerative compressor is considered a low specific speed machine, and in its normal range of specific speeds, its efficiency compares favorably with that of centrifugal compressors, although the latter are known to have a higher performance in some specific conditions. The regenerative compressors have a stable operation throughout the flow range and do not surge under any condition, and thus have advantages of stability over centrifugal compressors, which tend to surge at low flow rates. This characteristic of RFC compressors gives them an advantage since they do not surge even at zero flow, which makes stage matching less critical and off-design operation less restricted than with the centrifugal compressors. The volume of fluid in a centrifugal compressor is generally much higher than in a comparable regenerative compressor, and regenerative compressors have more ability to deliver fluid at a variable (desired) flow rate, which is something a centrifugal compressor lacks.

Another advantage of regenerative flow compressors is they generate less noise during their operation compared to centrifugal ones and their problems due to wear are minimal. That is why they are preferred in some applications, such as the emissions reduction in the automobile industry.

2.4 Pump Similarity Laws

The constraints on a turbomachine design in general, and pumps and compressors, in particular, are as diverse as the numerous applications. To estimate the performance of these machines and help design better ones, dimensional analysis is used to relate performance characteristics to the diameter, D, and the rotational speed, ω of the pump or compressor. These three dimensional parameters could also be used to estimate design and performance changes between two pumps or compressors of similar design. The dimensionless coefficients of the volume flow rate, Q, the total head, H, the power absorbed by the pump, P, will scale according to ϕ, ψ, and Π as follows.

Dimensionless flow coefficient: $$\phi = \frac{Q}{\omega \cdot D^3} \quad (1)$$

Dimensionless head coefficient: $$\psi = \frac{H}{\omega^2 \cdot D^2} \quad (2)$$

Dimensionless power coefficient: $$\Pi = \frac{P}{\rho \omega^3 D^5} \quad (3)$$

Typical performance characteristics of pumps and compressors both dimensionless and non-dimensionless are shown in Figures (19) and (20) below.

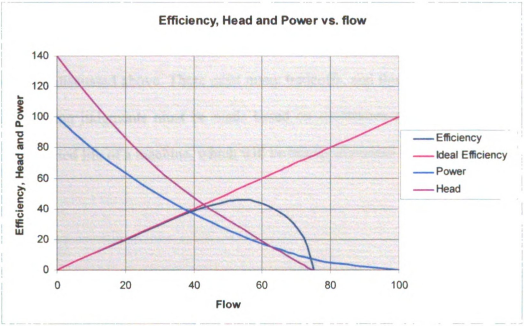

Figure 19: Performance Characteristics of Regenerative Compressor (after Iverson [5])

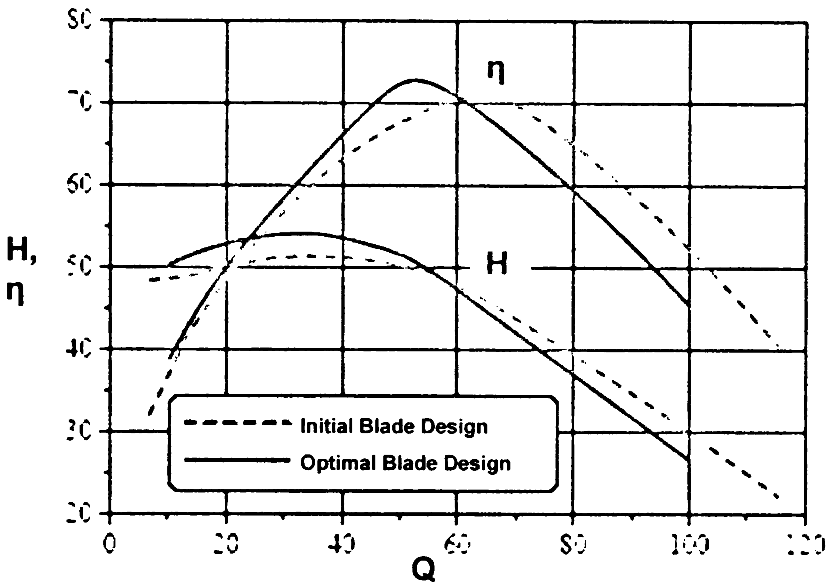

Figure 20: Pump characteristic curves with the initial and the optimal impeller (after John S. Anagnostopoulos 2005)

The design of a pump, compressor or turbine involves several factors other than the affinity laws discussed above. There exist many tradeoffs, and thus a lot of compromises and engineering judgments must be made based on constraints such as cost, reliability and the expected life of a machine, which will be briefly discussed in later chapters.

CHAPTER 3

LITERATURE SURVEY

3.1 Introduction

In the existing literature researchers have studied regenerative turbomachines as compressors, pumps, turbines, and blowers. In turbomachinery, most of the research has been performed on centrifugal pumps than on regenerative flow compressors and pumps. This literature could be broken down into three categories, including theoretical analysis, experimental work, and computational fluid dynamics. For the applications related to emission reduction and control, most of the research, especially experimental studies have been performed in the industry. Centrifugal flow compressors and pumps are widely used for automotive applications in external exhaust systems, and have been used for many decades. Only recently did regenerative flow compressors started to be used in such applications, because of some of their obvious advantages over the centrifugal turbomachines. Their late introduction into this type of application explains the limited literature available on these machines in comparison to their centrifugal counterparts.

3.2 Theoretical Models

Several theories have appeared in the literature concerning the principle of the operation of the turbomachines. While some of these theories have more solid arguments than others, most of them are worth mentioning because they address the different aspects of the flow mechanism inside the pump. Theoretical models, experimental work, and very modest CFD work compose the three major areas, in which some literature exists on regenerative flow compressors and pumps. The most important finding in this literature survey is that there does not exist one theory describing the flow and/or performance of regenerative flow compressors and pumps, which is completely independent of empirical data.

One of the researchers, Whitehead, experimentally investigated the performance of a Reavell RC50 regenerative compressor, and found a maximum aerodynamic efficiency of 44% occurring at a specific speed of 0.05. Whitehead, Harrison, and Rose [7] suggested an ideal mathematical model under the assumption of no loss for the diffusion process in an RFC. When these losses were incorporated into the equations, a reduction in the efficiency by more than 10 % was calculated at maximum speed. Whitehead also suggested that the performance of the compressor is affected to by Mach number, which turn out to not be supported by the experimental data, and the Reynolds number effects were found to be negligible. His predictions were not in good agreement with the experimental results. Hollenberg [8], on his side, studied regenerative pumps and blowers and reported the parameters controlling their efficiency. He conducted both theoretical and experimental analysis, and concluded that flow rate, pressure, and torque, are all dependent on one empirical parameter. He examined the effect of specific speed of turbomachines on efficiency, and showed that maximum efficiency is a function of friction head coefficient and radius ratio. Hollenberg also found that the optimum head and maximum efficiency were adversely affected by increasing the clearance between the impeller and stripper, and concluded that improved efficiency might be obtained at higher specific speeds.

Crewdson [9] and Iverson [10] developed the 'purely viscous' theory, in which they hypothesized that drag induced by the impeller on the stationary fluid in the side channel as being the crucial flow mechanism for pumping the flow through the pump. Iverson studied the performance of the pump, and developed equations considering a linear system with a linear motion of the fluid in contact with rough surfaces. He assumed a force balance on the fluid in the horizontal flow channel and applied newton's laws of fluid dynamics to derive performance equations of the pump. He analyzed the performance of regenerative pump in terms of shear stresses imparted to the fluid by the impeller. Some of the problems were that he had to assume an average impeller velocity, and another problem was that as a result of his theoretical analysis two shear coefficients were created, which had to be experimentally determined. Using a simplified approach similar to Iverson's, Balje [11] studied the regenerative flow turbine, and experimentally concluded that the optimum efficiency of a regenerative turbine is about 35%, which is less for regenerative pumps.

Seeno [12] studied the modeling of the internal flow of a radial blade impeller as Couette-Poiseuille flow under the condition of an adverse pressure gradient. His theory was based on the fact that turbulence is the main driving force of flow in the compressor. He developed a turbulence-mixing model, which considers a turbulent friction force as the pumping mechanism. Jakubowski [13] took a more theoretical approach by analyzing rotational flow of an incompressible, non-viscous fluid in a toroidal enclosure. His mathematical model was not very robust and could not be used due to the many assumptions he had to make to simplify solving his complex mathematical model.

Wilson, Santalo and Oelrich [14] postulated a helical flow pattern in the regenerative flow pumps and compressors as being their hypothesis. They hypothesized that this helical flow motion is a combination of two flow motions: a circulatory and a tangential flow motions. Their theory was based on the idea that the fluid gains angular momentum in the impeller and then imparts it to the slower moving fluid in the casing channel. The fluid then re-enters the impeller with a higher angular momentum, which is generated by the torque exerted on the fluid by the impeller.

Burton [15] presented a theoretical and experimental analysis of regenerative flow pumps and turbines. He developed expressions for turbomachine performance over entire operating range in terms of empirical constants. Burton also photographically recorded the helical flow pattern on which Wilson's developed his theory. He used an experimental machine where small-energized beads were introduced into the flow stream recorded their path.

Another theory was developed by Wright [10], which was named the momentum transfer theory. Wright's theorized that it is possible to increase the pump rotational speed without increasing the shutoff pressure rise, provided the blades were given a fitting backward curvature. He discovered that by curving the blades backwards by a proper angle, and increasing the rotational speed of the turbomachine, the same pressure rise was achievable. This finding disproves the purely viscous theory developed by Iverson and Balje.

Sixsmith [17] has designed and studied a regenerative flow compressor based on transfer of momentum theory. He designed an RFC with airfoil blades, which was more superior to its counterparts in generating more head rise. He designed the torus in such a way that allows the core to assist in guiding the fluid and circulates it through the blade passages with minimum losses. One of his main assumptions, however, was that he considered the deceleration of the flow in the channel to be a diffusion process.

It remains true that most of these theories were not extensive enough to take into consideration all of the design parameters, which affect regenerative flow turbomachines' performance. For instances, none of the theories account for all the losses, and if they do they oversimplify the problem to where it becomes application specific and cannot be generalized to encompass all regenerative flow compressors and pumps.

3.3 Experimental Work

The main concern of most of the researchers and developers of regenerative flow compressors has always been to study the effect of geometry design change on the turbomachine's performance. Many of them have experienced with changing the geometrical configuration and size of mainly the impeller, annular channel, and inlet and discharge ports.

Mason [18] carried out an experimental investigation of a regenerative pump with two channel diameters (2 inch and 1.25 inch), each with 40 and 20 blades in the pump impeller, where he compared experimental performance characteristics with a theoretical analysis of the fluid dynamic mechanism of regenerative pumps. He aimed at correlating empirical parameters with pump geometry, but his deductions were inconclusive.

In addition to his theoretical work on regenerative compressors and pumps, Senoo [19] experimentally investigated the influence of the inlet geometry configuration with respect to the rest of the pump components, on the characteristics of a regenerative pump. He stated that the pump performance could be significantly improved if the inlet port is appropriately located downstream from the barrier such that fluid entering the pump flow passage in a region where the impeller effect would be reasonably established. He stated that the fluid enters the pumping passage too far upstream when the inlet port is very close to the barrier where the impeller effect is not completely realized.

Shimosaka and Yamazaki [20] investigated the effects of varying the dimensions of the channel, impeller, and the clearances. They held some of the parameters constant while they established the effects of varying the different design parameters to study their effect on the pump performance. They concluded that the shear number of the design parameters involved would make it extremely difficult if not impossible to establish a complete method for the performance prediction of the regenerative flow pump. They resorted to systematic experimentation to prove the different design changes they put forward.

Crewdson [9] inspected the role of the circulatory flow or the centrifugal pumping in the process of enthalpy transfer in a regenerative pump. He divided the side channel of the pump into two parts. He then soldered a thin brass strip along the middle of the side channel, so that the flow is split into two sections one on each vertical side of the channel (upper and lower). He predicted that the circulatory flow, which is mainly radially inwards in the channel, would be greatly affected. What he found out was that although greatly hindered, the circulatory flow was not eliminated completely because there were still the centrifugal forces present. He also concluded that the reduction in the circulatory flow greatly reduced the pumping effectiveness.

Senoo [21] developed a theoretical model to study the effect of clearance on the pump performance in the case of radial blades. He carried out a series of experimental tests using a pump with radial blades. He changed the pump clearance eight to ten times from 0.04 mm to 0.36 mm and clarified the influence of the clearance experimentally and compared it with his theoretical results. In his experiment the shut-off head at large clearance was only one fourth of that at the small clearance. He found that the pump head depends a great deal on the value of pump clearance. A similar study on the effect of the stripper clearance on the overall pump performance was conducted by Abdallah [22], who suggested in his thesis that the performance of regenerative pump with airfoil blades might be improved if the solid stripper were modified to form a row of stationary blades to allow flow between the blades to continue in a toroidal rather than a peripheral path only. A four stage regenerative compressor was adopted by Gessner [23] for the compression of helium gas in the development of a highly reliable, long life cryogenic refrigerator for space vehicle application. The advantage of RFC is due to its ability to produce high-pressure ratio at low flow rate with a small overall size of machine. Further advantages are oil-free operation and freedom from stall or surge instability. These characteristics are advantageous in compressors intended for incorporation in small closed cycle helium refrigerators. There were further studies performed by other researchers in this area, but were not significant, in that they either were slight modifications of such previously developed theories, or did not have major contributions to better understanding the flow performance in regenerative pumps and compressors.

3.4 Numerical Simulation

Computational fluid mechanics is tool, which has become useful for fluid flow analysis in a wide range of machines and devices in all branches of the industry and academia. Because of the complex geometry of most of the turbomachines available, especially regenerative flow compressors and pumps, the restricted robustness of the numerical simulation software programs and difficulty of use, their use has been limited. As the computer processing power increased and the CFD software programs become more sophisticated, this tool's use has become more prevalent.

CFD helps get insight and understand the flow behavior inside these turbomachines, in addition to predicting their performance based on available design and operation parameters. An attempt to calculate the flow in regenerative turbomachines was undertaken by Abdallah [35], who applied an incompressible version of time marching scheme to the flow outside the blade row of a regenerative compressor with aerofoil blades. Andrew [36], by contrast proposed a method based on an adaptation of the streamline curvature technique commonly used for axisymetric through-flow calculations in conventional axial and radial flow turbomachines. Although this method did not calculate the details of the blade-to-blade flow, his work seems very attractive.

CHAPTER 4

DESIGN FORMULAE AND PROCEDURE

4.1 Introduction

The basic problem in the aerodynamic design of regenerative pumps/compressors is determining the maximum overall efficiency within certain limitations imposed by the type of application, and other considerations. Most of the research, which has been done so far, focuses on the direct problem, for which the focal point is to determine the flow parameters given the physical flow path and blading details. The less common, and more challenging approach, which has been broached lately by various researchers, is the indirect problem. The latter focuses on determining the optimum blade shapes, rotor diameter, and flow path geometry, given the flow parameters.

There are few mathematical models in literature, which explain the behavior of regenerative pumps and calculate their performance. Most of these models need extensive experimental support for performance prediction. For this reason, it is very important from an industrial point of view to find efficient theoretical models that can be used to predict the regenerative pump performance in more details. A relatively simple model for the Secondary Air Pump is chosen for study. The same exact analysis will be used to develop a mathematical model for similar air pump models.

4.2 Assumptions

A model with radial blades is adopted to perform this theoretical study. Only one side of the channel is considered.

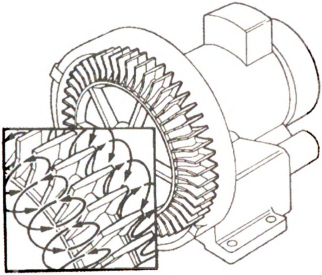

Figure 21: Regenerative pump (Adopted from [55])

In this theoretical analysis it is assumed that the flow has a helical path as shown in Figure (22), and that all the flow leaves the impeller at the tip of the blades.

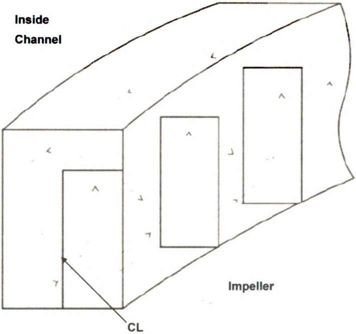

Figure 22: Helical Flow Path (as adopted from [24])

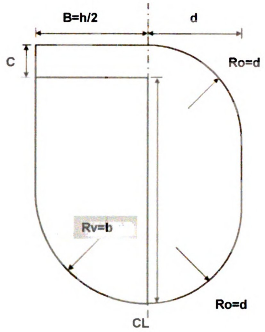

Figure 23: Simplified Design Channel Shape

4.3 Design Formulae

Approximate rules are required for the design of the most efficient pump with given limitations, so that the number of specific cases to be investigated can be kept to a minimum. Researchers have used different ways to design efficient RFP/RFC. Therefore the blade, amongst other things, greatly affects the transfer of energy from the rotor to the fluid. The basic energy transfer relation for all turbomachines including regenerative ones is a form of Newton's Second Law of motion, which is applied to a fluid traversing a rotor.

The change in magnitude of the radial velocity components through the rotor gives rise to a radial bearing load. The change in magnitude of the axial velocity components through the rotor gives rise to an axial force, which must be taken by a thrust bearing. Neither the radial nor the axial velocity components have any effect on the angular motion of the rotor, except for the effect of bearing friction. It is the change in magnitude and radius of the tangential components of velocity that corresponds to a change in angular momentum of the fluid and results in the desired energy transfer [25].

Blade number

Blade number (Z) is open to the designer to choose. The normal procedure is to make an initial choice of number of blades, and to change it later if needed [26]. If the blade number is too small, the fluid is poorly guided and energy transfer from the vanes to fluid decreases. On the other hand, if Z is too large, the skin friction increases, and the flow blockage depreciates machine performance. Previous experiments done by Badami [27] showed that the number of impeller blades has a direct effect on the head developed by the pump. For the purpose of this study, it is chosen to determine the number of blades by considering the aspect-ratio, which is the ratio of the vane pitch (spacing) to vane height.

$$K = \frac{2\pi . r_v \; / Z}{h \, / \cos(\beta_{in})} \tag{4}$$

Usual values for the vane aspect ratio for radial turbomachines are in the range: $0.35<K<0.45$. These values have also been used in the industry for regenerative pumps. The use of low-aspect-ratio compressors brings many benefits. Moore and Reid (1980) confirmed earlier studies that low aspect ratios produce higher peak pressure ratio, higher stage efficiency, and improved performance over the whole blade span. It also has good operation at higher incidences, and the blade's performance improves at high mach numbers.

The number of vanes is thus:

$$Z = \frac{2.\pi.r_v}{K.h} \cdot \cos(\beta_{in}) \qquad (5)$$

Substituting the radius of the vane's centroid into eqt.1 gives:

$$Z = \frac{4.\pi}{(\pi+4).K} \left[2.C_1 (r_2 / h) - C_2\right] \cdot \cos(\beta_{in}) \qquad (6)$$

For one-sided semicircular blade, $C_1 = C_2 = \frac{\pi}{2}$, and for radial vanes, $C_1 = \frac{\pi}{4} + 1$, $C_2 = \frac{3.\pi + 10}{12}$.

Blade thickness

A very thick vane causes large loss due to blockage effect, and moves circulating pivot to the inside of the open channel. On the other hand a thin vane moves the circulating pivot to the inside of the vane, and hence decreases the effectiveness of the circulating flow. Thus, it is important to find an optimum blade thickness. The circulating pivot has to be located on the line CL shown in Figure (23) in order for all circulating flow developed inside the channel to pass through the impeller.

$$t.Z = 2.\pi.r_2 \cdot \left\{ \frac{4.h}{C_1.r_2} \cdot \left(\frac{A_o.r_o}{h^3} - \frac{c.(r_2 + c/2)}{h^2} \right) + \frac{C_2.h}{2.C_1.r_2} \right\} \qquad (7)$$

Blade height

To guarantee that the circulating flow enters into the vane space smoothly, the vane height is determined by the following equation:

$$h = \left(r_2 - \frac{t.Z}{2\pi}\right) \cdot \frac{2\sqrt{\pi}}{\sqrt{Z} + \sqrt{\pi}} + \left(r_2 - r_c\right) \cdot \frac{\sqrt{Z} - \sqrt{\pi}}{\sqrt{Z} + \sqrt{\pi}} \tag{8}$$

Impeller inlet/outlet radii

The impeller inlet and outlet radii can easily be calculated as functions of the radial distance to impeller hub, circulatory flow, impeller tip and channel.

$$r_i = \sqrt{\frac{3}{10} \cdot \frac{4r_o^3 + 3r_o^2 r_c + 2r_o r_c^2 + r_c^3}{2r_o + r_c}} \tag{9}$$

$$r_e = \sqrt{\frac{3r_c^5 + 10r_2^2 r_3^2 (2r_3 - 3r_c) + 15r_2^4 r_c - 8r_2^5}{10(r_3 - r_c)^2 (2r_3 + r_c)}} \tag{10}$$

Stripper Clearance

The stripper is an isolating wall, which prevents the pressurized fluid in the outlet region from flowing into the inlet region at low pressure.

The clearance in a regenerative pump is usually taken to be less than 0.5% of the blade height ($\delta \leq 0.005h$).

$$\phi_l = \frac{Q_l}{Q_s} \tag{11}$$

$$\phi_l = \frac{\delta \cdot (h + b)}{A_o} \cdot \left[\frac{r_2}{r_o} + 2C_D \sqrt{\frac{2\theta_p}{Z_{st}} \cdot \frac{d\psi}{d\theta}}\right] - \frac{\delta h^2}{2A_o r_o} \tag{12}$$

A recommended value for Z_{st} is 3 to 5.

Stripper angle

More work is exerted on the fluid if the stripper angle is small, because of the increased pumping region.

$$\theta_{st} = \frac{t}{r_2} + \frac{2\pi\left(Z_{st} - 1\right)}{Z} \tag{13}$$

Slip-factor

Slip-factor is the ratio of the average peripheral velocity of the fluid leaving the impeller to the frame speed at the outlet of the impeller.

$$\sigma = \frac{\sigma_r + r_o \dfrac{\phi}{L_c}(1-\sigma_r)(1+\dfrac{Q_v}{Q_s})}{1+\dfrac{r_e}{L_c}(1-\sigma_r)(1+\dfrac{Q_v}{Q_s})} \tag{14}$$

Where, σ_r is the slip factor for radial turbomachinery. This radial slip-factor has been determined by Wilson [28] to be a function of the number of blades in the rotor and the blade angle at the rotor periphery.

$$\sigma_r = 1 - \frac{\sqrt{\cos\beta}}{Z^{0.7}} \tag{15}$$

4.4 Design Procedure

Input variables

Three input variables will be considered for the design procedure, and they are:

Design flow rate, design head rise, rotational speed.

The design variables are chosen to be tip gap, and channel aspect ratio.

Through iterative calculations by adjusting the design variables (c, AR), other geometric variables are found to produce the design flow rate and head at its maximum efficiency.

A design procedure flow-chart is developed and is as follows:

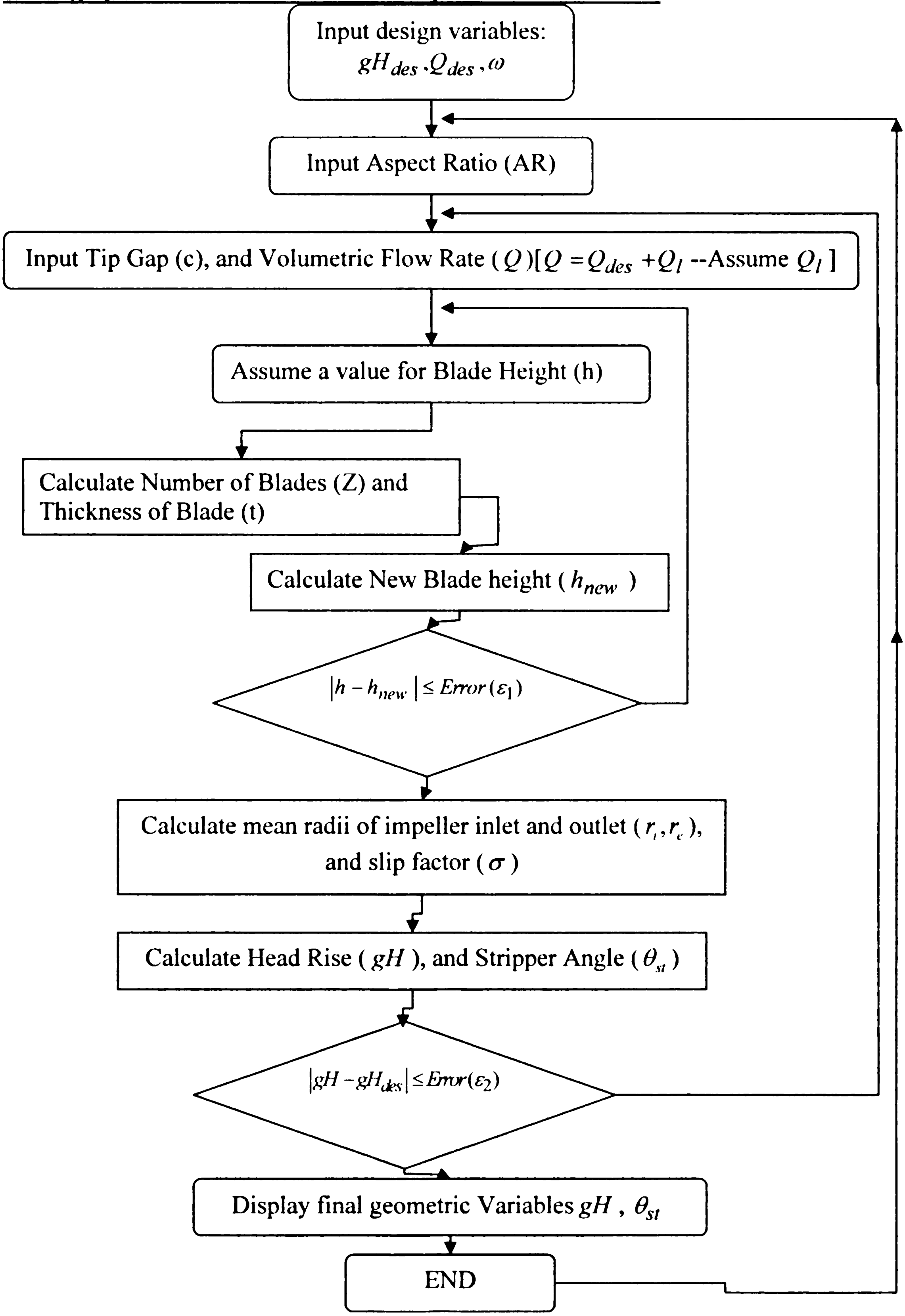

4.5 Performance

The variables used to evaluate the performance of the rotor of the RFP are efficiency and head rise.

Efficiency

A wide variety of efficiency definitions exist that describe the thermal, volumetric, and energetic qualities of a pump/compressor. Because of the difficulty in accurately measuring experimental suction and discharge temperatures, these forms of efficiency tend to be erroneous. Different studies [29] have used overall efficiency to evaluate RFP/RFC performance. The overall efficiency is defined as the ratio of an adiabatic or isothermal power to shaft power. Moreover, adiabatic efficiency value is the appropriate measurement of performance for a mechanical pump or compressor system. Thus the overall adiabatic efficiency is suitable for the study of the air gas pump. To be more accurate and account for the change (decrease) in mass flow in a reported efficiency, the specific adiabatic overall efficiency is considered. The latter is the adiabatic overall efficiency per unit mass.

The adiabatic (overall) efficiency is equivalent to the product of mechanical efficiency and isentropic efficiency. Adiabatic efficiency is equal to isentropic efficiency if and only if the mechanical efficiency is unity (100%) [30]; this means that there must be no heat rejected from the pump/compressor for this to be true. For such a case, the pump/compressor surface would be at the same temperature as the ambient. The specific adiabatic overall efficiency is expressed by:

$$\bar{\eta}_{overall,ad} = \frac{\dot{m}_{\exp} c_p T_i \left[\left(\frac{P_o}{P_i} \right)^{\frac{k-1}{k}} - 1 \right]}{\dot{W}_{shaft,\exp}} \qquad (16)$$

Where, $\dot{m}_{\exp}$ is the experimental discharge mass flow, T_i is the ambient inlet temperature, $\frac{P_o}{P_i}$ is the theoretical pressure ratio, and $k = 1.4$

Head rise

$$\psi = \frac{gH}{U_o^2} \qquad (17)$$

and

$$\psi_c = \frac{\vartheta Q_c}{Q_s} \left[\sigma \left(\frac{r_e}{r_o} \right)^2 - \alpha \left(\frac{r_i}{r_o} \right)^2 \right] \qquad (18)$$

$$\Delta \psi_\theta = \frac{\Delta g H_\theta}{U_o^2} \qquad (19)$$

Where ψ_c denotes the head rise due to the increase of angular momentum of the circulatory flow in the pumping region. ϑ is the effectiveness of the circulatory flow rate and denotes the substantial circulatory flow rate passing through the impeller ($\vartheta = 1$) in the case if the circulatory pivot is on the CL line as shown in Figures (22 and 23). $\Delta \psi_\theta$ denotes the head loss due to the tangential flow passing through from the inlet to outlet ports; it is evaluated by the classical pipe friction loss formula [31].

CHAPTER 5

FLUID DYNAMIC ANALYSIS OF RFP/RFC

5.1 Introduction

The mechanism of operation of the secondary air pump is described in terms of a circulatory flow (meridional flow), Q_C , superposed on a tangential (through flow), Q_T . The through flow is the integral of the product of the tangential velocity and the differential area over the area of the open channel.

The major quantities which describe the operation of the ideal model of the air pump are the flow rate (Q) or capacity, Total Head (H), Hydraulic Efficiency (η), circulatory flow (Q_C), work input to fluid (W_{in}).

The equations derived for an ideal model, which is restricted to specific assumptions and known facts and with the influence of friction. Theoretical equations for total head and efficiency are developed for this model pump. CFD and experimental data for the actual model are compared.

The concept of the ideal model is introduced because the solutions to the differential equations representing the flow in the pump, assuming they can be obtained, would be very complicated to use in an engineering solution. Thus the three-dimensional motion of the fluid flow can be described generally in qualitative statements.

5.2 Tangential Pressure Rise

The angular Momentum applied to the control volume shown in Figure 24:

$$\int_A \Pr dA - \int (P + \frac{dP}{d\theta}) r dA = \rho dQ_C \left(\alpha r_1 U_1 - \sigma r_2 U_2\right) \tag{20}$$

Simplifying and using the assumptions, we get:

$$\frac{dP}{\rho} = \frac{dQ_C \omega\left(\sigma r_2^{\,2} - \alpha r_1^{\,2}\right)}{A r_g} - g dH_{ts} \tag{21}$$

Where σ is the slip factor defined as the ratio of the tangential velocity of fluid to impeller velocity at periphery of rotor (Point 2 in Figure 23), and α is the ratio of the tangential velocity of fluid to impeller velocity at blade base (point 1 in Figure (24).

H_{ts} is the head loss due to tangential shear forces on the open channel wall. For simplicity in the analysis, wall friction and other irreversibilities are included as head losses.

$$V_{t1} = \alpha U_1 \quad \text{and} \quad U_1 = r_1 \omega \tag{22}$$

$$V_{t2} = \sigma U_2 \quad \text{and} \quad U_2 = r_2 \omega \tag{23}$$

$$dQ_C = b.r_2 V_{C2}.\cos(\gamma) d\theta = y.r_1 V_{C1} d\theta \tag{24}$$

Using the assumption that the tangential pressure gradient is independent of the radius, and letting:

$$r_g A = \int_A r dA \tag{25}$$

We get equation (21) above for tangential pressure rise.

5.3 Tangential Flow Equation

The tangential pressure gradient and the mass flow rate of the circulatory flow are independent of radius.

Applying the second law on the abovementioned control volume, gives the differential equation between points 2 and 3:

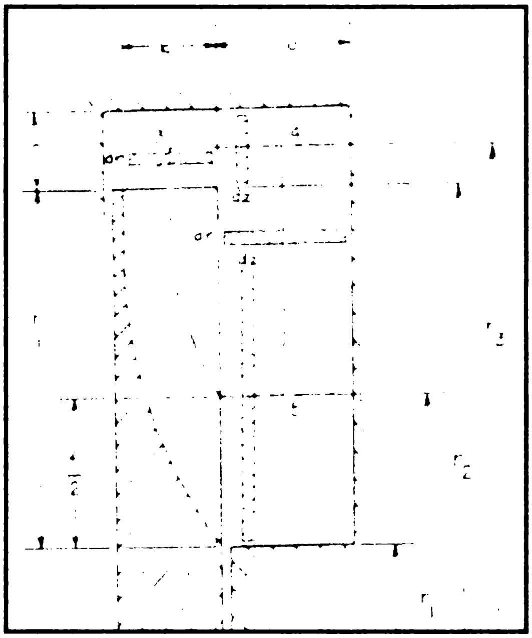

Figure 24: Open Channel and Impeller Dimensions [26]

$$\frac{\partial V_t}{\partial r} + \frac{V_t}{r} = -\frac{b}{\rho}\frac{\partial p}{\partial \theta}\frac{d\theta}{dQ_C} \tag{26}$$

The expression of the tangential velocity between points 2 and 3 is the solution to the above D.E.

$$V_{t(2\to 3)} = \frac{\sigma r_2 U_2}{r} - \frac{b}{2}\frac{\partial p}{\partial \theta}\frac{d\theta}{d\dot{m}_c}\frac{r^2 - r_2^2}{r} \tag{27}$$

Where $d\dot{m}_c = \rho dQ_c$

Similarly, considering a differential control volume between points 3 and 4, and using the angular momentum in the tangential direction, we get the following equation of motion:

$$\partial V_t = c\frac{\partial p}{\partial \theta}\frac{d\theta}{d\overset{\bullet}{m}_c}dz \qquad (28)$$

Noting that the pressure gradient and the mass flow rates are independent of z, and using the equation (28) above to determine V_{t3}, we get,

$$V_{t(3\to 4)} = \frac{\sigma.r_2U_2}{r_3} - (\frac{\partial p}{\partial \theta}\frac{d\theta}{d\overset{\bullet}{m}_c})(c(z_3 - z) + b(\frac{r_3^2 - r_2^2}{2r_3})) \qquad (29)$$

Applying Newton's law in terms of angular momentum to the control volume between points 4 and 5 we get the equation of motion of the fluid in this differential volume:

$$\frac{\partial V_t}{\partial r} + \frac{V_t}{r} = d\frac{\partial p}{\partial \theta}\frac{d\theta}{d\overset{\bullet}{m}_c} \qquad (30)$$

Solving the D.E., substituting the expression for V_{t4}, and letting the length between points 3 and 4 be $d_{3,4}$, we obtain:

$$V_{t(4\to 5)} = \frac{\sigma.r_2U_2}{r} - (\frac{\partial p}{\partial \theta}\frac{d\theta}{d\overset{\bullet}{m}_c})\left[b(\frac{r_3^2 - r_2^2}{2r}) + \frac{c.r_3d_{3,4}}{r} + d(\frac{r_3^2 - r^2}{2r})\right] \qquad (31)$$

Between points 5 and 1, which complete the cycle of the circulatory flow in each passage between two successive blades, the equation of motion is:

$$\partial V_t = -\frac{\partial p}{\partial \theta}\frac{d\theta}{d\overset{\bullet}{m}_c}fdz \qquad (32)$$

$$V_{t(5\to 1)} = \frac{\sigma.r_2U_2}{r_1} - (\frac{\partial p}{\partial \theta}\frac{d\theta}{d\overset{\bullet}{m}_c})\left[f(\frac{r_3^2 - r_2^2}{2r_1}) + \frac{c.r_3d_{3,4}}{r_1} + d(\frac{r_3^2 - r_1^2}{2r_1}) + f(z - z_5)\right] \qquad (33)$$

The last four equations of velocity represent the through flow velocity profile of the ideal model along the separate segments of the projection of a mean line on the meridional plane. Integrating these equations and summing up, we obtain an expression for the tangential of through flow along the linear section of the channel (equation (34) below).

$$Q = \sigma r_2 U_2 \left[b \ln(r_3/r_4) + d \ln(r_3/r_1) + \frac{A_2}{r_3} + \frac{A_4}{r_1} \right] - \left(\frac{\partial p}{\partial \theta} \frac{d\theta}{d\dot{m}_c} \right) \left[\begin{array}{l} \frac{(r_3+r_2)A_1}{2}\left(\frac{b}{2}+\frac{A_2}{r_3}+\frac{A_4}{r_1}\right) - \\ \frac{(r_3+r_1)A_3}{2}\left(\frac{A_4}{r_1}-\frac{d}{2}\right)+\frac{A_2^2}{2}+\frac{A_2 A_4 r_3}{r_1}+ \\ \frac{A_4^2}{2}-\left(\frac{b^2 r_2^2}{2}\ln(\frac{r_3}{r_2})\right)+ \\ \ln(\frac{r_3}{r_1})\left(d r_3 A_2+\frac{d^2 r_3^2}{2}+\frac{d(r_3+r_2)}{2}\right) \end{array} \right]$$

5.4 Circulatory Flow Losses

More than 40% of the input power in a regenerative turbomachine is consumed in overcoming losses. Different types of losses affect the regenerative pump operation including:

- Hydraulic losses in the circulation process between impeller and free channel
- Peripheral friction loss in the flow channel
- Losses due to slip
- Inlet and outlet losses
- Leakage losses between the impeller face and the pump casing and between the inlet and outlet ports through the stripper, but there insignificant due to their fine clearances achievable with RFC/RFP.

The circulatory losses are discussed in this section, while the other losses are addressed in subsequent sections.

Channel

The energy equation is applied to the control volume shown in Figure (25), and steady flow is assumed to the circulatory flow. The meridional pressure drop in the open channel is obtained as follow.

$$\frac{P_2 - P_1}{\rho} = \left(\sigma r_2{}^2 - \alpha r_1{}^2\right)\frac{Q\omega}{Ar_g} + \frac{1}{2}\alpha^2 U_1{}^2 - \frac{1}{2}\sigma^2 U_2{}^2 + \frac{1}{2}V_{C1}{}^2 - \frac{1}{2}V_{C2}{}^2 + gH_{lc} \qquad (35)$$

Where, H_{lc} accounts for the irreversilbilities in the open channel.

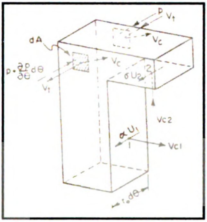

Figure 25: Section of the open channel's control volume [26]

The angular momentum equation when applied to the control volume in Figure (25), gives the expression:

$$dT = \rho dQ_C\left[\sigma r_2 U_2 - \alpha r_1 U_1\right] + aR\frac{dP}{d\theta}d\theta \qquad (36)$$

Where the torque differential dT is a function of the power differential dP:

$$dP = \omega \cdot dT \qquad (37)$$

Thus the power input differential:

$$dP = a\omega R dp + \rho dQ_C\left[\sigma U_2{}^2 - \alpha U_1{}^2\right] \qquad (38)$$

Where dp is the pressure difference.

Impeller

Using Berboulli's equation to the control volume of the impeller shown in Figure (25), we get the following expression for the meridional pressure:

$$\frac{P_2 - P_1}{\rho} = \left(\sigma U_2{}^2 - \alpha U_1{}^2\right) + \frac{1}{2}\alpha^2 U_1{}^2 - \frac{1}{2}\sigma^2 U_2{}^2 + \frac{1}{2}V_{C1}{}^2 - \frac{1}{2}V_{C2}{}^2 - gH_{li} \tag{39}$$

Where, H_{li} represents the loss due to the passage of the circulatory flow through the impeller.

Equating the above two equations and simplifying, we get the total head loss in the circulatory flow.

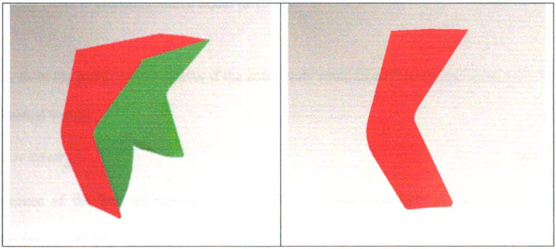

Figure 26: Section of the impeller's control volume - Blade Passage

$$gH_{Tc} = gH_{lc} + gH_{li} \tag{40}$$

$$gH_{Tc} = \left[\frac{Q}{\omega r_G A} + 1\right]\left(\alpha r_1{}^2 - \sigma r_2{}^2\right)\omega^2 \tag{41}$$

5.5 Theoretical Total Head

For this air pump, we are interested in the total head developed volume rate of flow of the fluid pumped. The pressure rise and the mass flow rate are of interest as well. The head is the net mechanical energy added to the fluid in the pump.

Considering the radial or circulatory flow Q_C for half the pump, and the change over the angle theta of the working section of the pump, the theoretical total head rise developed by the ideal model is defined as:

$$\Delta H = \frac{Q_C\left(\sigma r_2 U_2 - \alpha r_1 U_1\right)}{A r_g} \tag{42}$$

Note:

In the case of a rotor, which has an infinite number of blades of infinitesimal thickness, the slip factor σ can be assumed equal to 1.

The flow the pump would deliver if the solid body rotation with respect to rotor velocities obtained were Q_s.

$$Q_s = 2A\omega r_g \tag{43}$$

Because of the loss of mechanical energy by mechanisms such as wall friction and turbulence, the total head, as determined by measurement, is less than the head computed using equation (42) above. Considering the inlet and discharge losses, the general expression for head rise will be:

$$\Delta H = H_T + \Delta H_f \tag{44}$$

Where H_T is the actual total head developed by the pump, and H_f is the term representing the head loss. This loss term includes the inlet and outlet discharge losses, irreversibilities through the stripper associated with the turbine work, and head drop through the working section. Assuming that the radial and tangential losses are proportional to the square of the flow, Wilson assumed a constant of proportionality $k_t \approx 2000$.

$$\Delta H_f = k_t Q^2 \tag{45}$$

5.6 Hydraulic Efficiency

In the impeller or casing passages, the flow is accompanied by frictional losses. All losses convert mechanical energy into thermal energy. Wall friction effects, for instance, by viscous forces and by turbulence generation cause direct dissipation of energy. Secondary flow losses occur in regions of flow separation, where circulation is maintained by external flow and in curved flow passages where it is maintained by centrifugal effects.

Although, the practical performance parameter as determined by test is the overall pump efficiency, the mechanical energy losses discussed above are accounted for by considering the hydraulic efficiency.

$$\eta = \frac{Q}{Q_s} \tag{46}$$

Including loss terms, the efficiency is expressed as

$$\eta = \frac{Q}{Q_s}\left(\frac{H_T}{H_T + H_f}\right) \tag{47}$$

In this chapter the concept of the ideal model is introduced because the solutions to the differential equations representing the flow in the pump, assuming they can be obtained, would be very complicated to use in an engineering solution. The three-dimensional motion of the fluid flow is generally described in qualitative statements. Tangential pressure rise, tangential and circulatory flow equations are developed, and expressions for head and efficiency are derived.

CHAPTER 6

EXPERIMENTAL AND CFD METHODOLOGY

6.1 Introduction:

The process of designing pumps in particular and turbomachines in general, is very seldom straightforward. The final design is usually the result of many compromises, which involve several engineering disciplines such as fluid dynamics, mechanical design, and manufacturing.

Flow in pumps is a complex 3D phenomenon that includes turbulence, secondary flows, and unsteadiness. A substantial amount of pressure and efficiency gains can be obtained from a good understanding of the exact flow mechanism and associated losses, which include hydraulic, shock, leakage, suction and discharge, and peripheral friction losses.

CFD has been shown by many researchers to be an effective and efficient design tool. In the industry CFD has become a major element in the aero-design of turbomachines, and its applicability to more and more complex numerical models.

The mathematical formulation of fluid dynamics is based on a conservation of mass, momentum, energy, and entropy. The momentum equations are the Reynolds-averaged Navier-Stokes equations including (x, y, and z momentum). Energy equations are especially considered when heat transfer is involved. In addition depending on the complexity of the problem, such as the presence of turbulence, other equations are considered. There is a strong motivation to preserve these conservation properties when making numerical approximations.

The CFD package chosen for this study is a product of Fluent, Inc. and consists of a preprocessor called GAMBIT and a set of flow solvers customized to various flow situations. In this research, GAMBIT was utilized to define the solution domain, generate a mesh suitable for the pump assembly, and specify boundary zones, which include the impeller, inlet, outlet, and torus. The flow solver used in this analysis is FLUENT 5, which was selected for flow computations in this study, because it offers complete unstructured mesh flexibility, and non-conformal mesh interface capabilities, making it suitable for the secondary air pump application in hand, which involves complex flow geometry.

Another software package used in this study for numerical flow simulation is STAR CCM+. This package is more robust than FLUENT in meshing a relatively complex geometry such as that of an RFC.

6.2 Model Meshing

The flexibility of the computational mesh structure is tied to the adaptability and accuracy of the thermo-fluids analysis system. This determines both the level of geometrical complexity it can handle and the degree of control it offers over resolution of flow features. The function of the mesh is to fit the boundary surface of the computational domain and subdivide its volume into subdomains (cells), used in the numerical solution of the differential conservation equations of the mathematical model.

In the literature, both structured and unstructured grid concepts have been used for CFD simulations. For turbomachinery applications, most components in regular shape can be meshed with high-quality structured grids. However, in some components or local areas, such as casing treatments, or tip clearance, very often it is not easy to generate structured grids even with a multi-block topology. During the past decade the unstructured-grid methods have shown that they are promising in turbomachinery applications [37] and [38]. Nowadays the structured CFD solvers are still popular within the design loop of turbomachines although they are restricted in their geometric flexibility.

Traditional turbomachinery analysis demands the highest quality mesh for the least number of nodes, which usually translates into a hexahedral or a tetrahedral meshing strategy. Both Fluent and STAR CCM+ have these meshing capabilities.

For large turbomachine analysis, such as the one undertaken in this study where a 3-dimentional fluid flow analysis is sought after, it is desirable to create mesh in logical sections corresponding to the main geometrical components, rather than create one large mesh for the entire machine. With this in mind, the author set out to mesh RFC models using this meshing strategy. The appropriate meshing strategy is comprised of several steps. These include meshing the impeller air mass, which has the largest number of surfaces and bodies. Then meshing the torus represented by one body, which includes inlet and outlet surfaces as seen in Figure (27). Different cell shapes, including hexahedron and tetrahedron, and polyhedron were used for volume discretization to control mesh spacing within the solution domain interior so that the density of the mesh is high in blade passage and near-wall regions where gradients of the flow variables are steep, and the mesh is not as fine in areas where characteristics change less rapidly. The mesh spacing, non-orthogonality, and time-step size were controlled to minimize the discretization error, and ultimately reduce errors in the final simulation results.

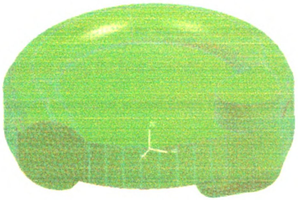

Figure 27: Meshed air mass of an air pump (Showing joined torus and impeller air-mass)

6.3 Model Preparation and Processing

Turbomachinery simulations typically provide steady (time-averaged) solutions of either Navier-Stokes (viscous), or Euler (inviscid) equations. Turbomachinery flow fields are three-dimensional in nature and highly complex. Flows are predominantly viscous and turbulent, and mostly compressible, and may range from subsonic to supersonic, where the rotation is a major factor influencing the flow behavior. Much of the complexity of turbomachinery flow fields is directly influenced by component geometry and flow-path. A good and methodical understanding of flow-path geometry and the effects of the different components of the turbomachine allows designing a better performing machine, in this case a RFC.

The set of equations solved in each simulation included the continuity equation, the Reynolds-averaged Navier-Stokes equations (x, y, and z momentum), the energy equation, and the chosen turbulence model equations. All simulations were calculated using the steady-state segregated, implicit solver formulation. This formulation employs a pressure-correction scheme whereby the momentum equations are solved sequentially for the velocity components using the best available estimate for the pressure distribution. Subsequently, the pressure correction is calculated from a derived Poisson equation, and the process is repeated until the continuity equation is satisfied. The pressure-correction scheme utilized for the simulations reported herein is called SIMPLE (Semi-Implicit Method for Pressure-Linked Equations). The SIMPLE algorithm provides the necessary coupling between the calculated velocity field and the pressure field for segregated solution of the governing equations.

The differential equations governing the conservation of mass, momentum, energy, etc. within the fluid are discretized by the finite volume (FV) method. To ensure that the discretized forms preserve the conservation properties of the parent differential equations, they are first integrated over a finite time increment, and then approximated in terms of the cell-centred nodal values of the dependent variable. Second-order discretization of the governing equations was used for all computations. Fluent provides many different turbulence models from which to choose, including the standard k-ε model, which was used extensively throughout the numerical simulation undertaken in this study along with other models. The turbulence model selected for the current investigation is the standard k-ε model, which is derived from the Reynolds-averaged equations, and gives rise to an additional term in the model equation of turbulence dissipation. In a study by Hermanson and Thole (1999), the predictive capabilities of the standard k-ε model were benchmarked against experimental velocity data taken by Kang et al. (1998) in the stagnation plane of a turbine vane. Calculations using k-ε were found to give good agreement with experimental data.

Pre-processing, Processing, and Post-processing

Pre-processing refers to all the steps, after mesh generation, required to prepare a CFD simulation: selection of mesh or meshes, definition of fluid properties and flow physics, specification of boundary conditions. Processing is the actual numerical simulation, which takes place solving the different discretized PDE's and obtaining converged solutions, which could be interpreted later in the post-processing phase. Different parameters are used and keyed in the solver in order to run and monitor the progression of the processing stage and the solution. If the solution converges and the performance characteristics are verified and validated, then the results could be represented in different formats as contours, 2D or 3D plots and graphs. Variables such as dynamic pressure, average velocity, and turbulence could be plotted at any part or stage of the flow volume, which was simulated. An example of an air-mass volume flow, which was meshed and ready to be simulated, is shown in Figure 28.

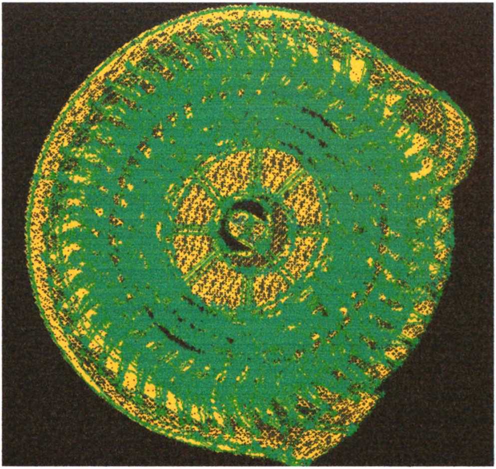

Figure 28: Meshed air-mass for an RFC pump

Many steps are involved in the preparation of the model for the three abovementioned processing phases. In this study some of the main processing steps are explained below. It is also important to mention that in this study air with specific boundary conditions at the suction, discharge of the pump, and the impeller air-mass are used.

<u>Boundary Conditions:</u>

Pressure and Velocity boundary conditions are important to specify in the CFD simulations run by the author during this study. For pressure boundary conditions for instance, there are typically two types, referred to as stagnation and static pressure conditions. A stagnation pressure condition assumes stagnation conditions outside the boundary so that the velocity at the boundary is zero. This assumption requires a pressure drop across the boundary for flow to enter the computational region. In contrast, in a static condition the pressure is more or less continuous across the boundary and the velocity at the boundary is assigned a value based on a zero normal-derivative condition across the boundary. Since the static pressure condition says nothing about fluid velocities outside the boundary, other than it is supposed to be the same as the velocity inside the boundary, it is less specific than the stagnation pressure condition. The ability to specify a pressure condition at one or more boundaries of a computational region is an important and useful computational tool.

Relaxation and Convergence Criteria

Numerical methods used to solve the equations for fluid flow and heat transfer most often employ one or more iteration procedures. By their nature, iterative solution methods require convergence criteria that are used to decide when the iterations can be terminated. In many cases, iteration methods are supplemented with relaxation techniques. Selecting proper relaxation and convergence criteria can be a difficult and frustrating experience for users of computational fluid dynamics (CFD) software. The criteria depend on the specifics of the problem being solved, and they may change during the evolution of a problem. Unfortunately, there are no universal guidelines for selecting criteria because they depend not only on the physical processes being approximated, but also on the details of the numerical formulation.

For example, over relaxation is often used to accelerate the convergence of pressure-velocity iteration methods, which are needed to satisfy an incompressible flow condition. Under-relaxation is sometimes used to achieve numerically stable results when all the flow equations are implicitly coupled together. The amount of over or under relaxation used can be critical. Too much leads to numerical instabilities, while too little slows down convergence. Similarly, a poorly chosen convergence criteria can lead to either poor results (when too loose) or excessive computational times (when too tight).

Although the two numerical simulation programs used by the author, namely FLUENT and STAR CCM+, have a standard set of recommended criteria, the author had to often resort to trial-and-error adjustments to get good results.

Implicit /Explicit Method

Numerical solution schemes are often referred to as being explicit or implicit. The computation is said to be explicit when a direct computation of the dependent variables can be made in terms of known quantities. On the contrary, when the dependent variables are defined by coupled sets of equations, and either a matrix or iterative technique is needed to obtain the solution, the numerical method is said to be implicit. The principal reason for using implicit solution methods, which require more computational effort in each solution step, as was the case in this study, is to allow for large time-step sizes. Numerical stability has to do with the behavior of the solution as the time-step dt is increased. If the solution remains well behaved for arbitrarily large values of the time step, the method is said to be unconditionally stable. This situation never occurs with explicit methods, which are always conditionally stable.

In computational fluid dynamics, the governing equations are nonlinear and the number of unknown variables is typically very large. Under these conditions implicitly formulated equations are almost always solved using iterative techniques. Iterations are used to advance a solution through a sequence of steps from a starting state to a final, converged state. This is true whether the solution sought is either one step in a transient problem or a final steady-state result. In either case, the iteration steps resemble a time-like process, although the iteration steps usually do not correspond to a realistic time-dependent behavior. It is this aspect of an implicit method that makes it attractive for steady-state computations, because the number of iterations required for a solution is often much smaller than the number of time steps needed for an accurate transient that asymptotically approaches steady conditions.

For the aforementioned reasons, in all of the simulation runs undertaken for the secondary air pump, the implicit method was used.

Incompressibility:

All materials, whether gas, liquid or solid exhibit some change in volume when subjected to a compressive stress. The degree of compressibility is measured by a bulk modulus of elasticity, E, defined as either $E=dp/(d\rho/\rho)$, or $E=dp/(-dV/V)$, where dp is a change in pressure and dr or dV is the corresponding change in density or specific volume. Since $dp/d\rho=c^2$, where c is the adiabatic speed of sound, another expression for E is $E=\rho c^2$.

In liquids and solids E is typically a large number so that density and volume changes are generally very small unless exceptionally large pressures are applied. If an incompressible assumption is made in which densities are assumed to remain constant, it is important to know under what conditions that assumption is likely to be valid. There are, in fact, two conditions that must be satisfied before compressibility effects can be ignored.

A simple way to define incompressibility with a good approximation when the ratio d r /r is much smaller than unity. To determine the conditions for this approximation we must estimate the magnitude of changes in density. In steady flow, the maximum change in pressure can be estimated from Bernoulli's relation to be $dp=\rho u^2$. Combining this with the above relations for the bulk modulus, we see that the corresponding change in density is $d\rho/\rho = u^2/c^2$ (1). Thus, the assumption of incompressibility requires that fluid speed be small compared to the speed of sound, Condition One: $u << c$. In unsteady flow another condition must also be satisfied. If a significant change in velocity, u, occurs over a time interval t and distance l, then momentum considerations (for an inviscid fluid) require a corresponding pressure change of order $dp = \rho ul/t$. Since changes in density are related to changes in pressure through the square of the sound speed, $dp=c^{2d\rho}$, this relation becomes $d\rho/\rho = (u/c)l/(ct\ )$.

(2) Comparing with expression (1), we see that the factor multiplying (u/c) must also be much less than one, Condition Two: $l << ct$. Physically, this condition says that the distance traveled by a sound wave in the time interval t must be much larger than the distance l, so that the propagation of pressure signals in the fluid can be considered nearly instantaneous compared to the time interval over which the flow changes significantly. An example of why both conditions are required can be found in the collapse of a vapor bubble. During the collapse process the surrounding liquid can be treated as an incompressible fluid because the collapse velocity is much less than the speed of sound.

However, at the instant the bubble vanishes, all the fluid momentum rushing toward the point of collapse must be stopped. If this really happened instantaneously, the collapse pressure would be enormous, i.e., much larger than what is actually observed. Since a sound signal requires time to travel out from the collapse point to signal incoming fluid that it must stop, Condition Two is violated (i.e., $l > ct$). An accurate numerical model of the collapse process, one capable of predicting the correct pressure transients, requires the addition of bulk compressibility in the liquid.

In all of the CFD simulations used in this study, air is assumed to be incompressible.

Turbulence:

The majority of flows in nature are turbulent. Because of this fact the question is often raised whether it is necessary to include some representation of turbulence in computational models of flow processes. Unfortunately, there is no simple answer to this question and the modeler must exercise some engineering judgment. $R_e = \rho UL / \mu$

Where r is fluid density and m is the dynamic viscosity of the fluid. The parameters L and U are a characteristic length and speed for the flow. The choice of L and U are somewhat arbitrary and there may not be single values that characterize all the important features of an entire flow field. The important point to remember is that Re is meant to measure the relative importance of fluid inertia to viscous forces. When viscous forces are negligible the Reynolds number is large.

The actual value of a critical Reynolds number that separates laminar and turbulent flow can vary widely depending on the nature of the surfaces bounding the flow and the magnitude of perturbations in the flow. Roughly speaking, a Reynolds number above

2500 is probably turbulent, while a Reynolds number below 1000 is not. In a fully turbulent flow there exist a range of scales for fluctuating velocities that are often characterized as collections of different eddy structures. If L is a characteristic macroscopic length scale and l is the diameter of the smallest turbulent eddies, defined as the scale on which viscous effects are dominant, then the ratio of these scales can be shown to be of order $L/l \gg Re^{3/4}$. This relation follows from a steady-state assumption that the smallest eddies must dissipate into heat the turbulent energy being generated in the flow. From the above relation for the range of scales it is easy to see that even for a modest Reynolds number (i.e. $Re=10^4$), the range spans three orders of magnitude, $L/l=10^3$. In this case the number of control volumes needed to resolve all eddies in a three-dimensional computation would be greater than 10^9. Numbers of this size are well beyond current computational capabilities. For this reason considerable effort has been devoted to the construction of approximate models for turbulence. The software programs used in this study namely FLUENT and STAR CCM+ have some of these capabilities.

The distinction between laminar and turbulent flow lies in the ratio of the inertial transport to the viscous transport. As this ratio increases, instabilities develop and velocity fluctuations begin to occur. A turbulent model accounts for the effect of these fluctuations on the mean flow by using an increased viscosity, the effective viscosity, in the governing equations. The effective viscosity is the sum of the laminar viscosity (which is a property of the fluid) and turbulent viscosity (which is calculated from a turbulence model), $\mu_e = \mu + \mu_t$, and generally, the more turbulent the flow field, the higher the effective viscosity. In this study, both laminar and turbulent assumptions were made to perform the numerical simulations, and the results were determined to be relatively close.

6.4 Experimental Approach and Validation of CFD Results

The experimental work was conducted for the regenerative flow compressors and pumps using testing apparatus to measure the different performance characteristics, such as flow and head. Two different set-ups are used for testing, manual and automatic. The input parameters, such as the pressure at the inlet and outlet, rpm, and current draw are controlled and the performance characteristics are recorded. Different prototypes for the secondary air pump have been built and tested. The inlet and outlet pressures are set to 0Kpa and 10Kpa gauge respectively. The prototype pump is run by an electric motor, for which the operational rotational speed range varies from 0 to 20,000 rpm. Room temperature is used throughout the entire test.

Other tests are also performed on the pump, where the temperatures could vary largely from the standard room temperature. Tests, such as the durability test, where temperature of operation ranges from –30 C to 120 C.

A prototype of an electric air pump is often built using Stereolithography (SLA), which turns a 3D CAD drawing of each one of the air pump components, namely the impeller, housing, and cover, into a solid object (an SLA unit is similar to a production part such as the one shown in Figure 29). These components are then built into pumps by integrating all the other different components as shown in Figures 13 and 14. The pumps are then tested for performance using both manual and automatic flow testing apparatus, where rpm and back-pressure are set and flow and current draw are measured. One of the main assumptions made in developing the analytical model was the linearity of the pressure rise inside the channel or torus area of the pump. A test has been designed to test the validity of this assumption, and the results are shown in Figure 30. To measure pressure, pressure sensors were imbedded in both the cover (upper) and housing (bottom) parts of the pump along the torus at 45^o increments from the suction all the way around the pump [0^o – 315^o], excluding the stripper region. It is clearly seen from Figure 30 that flow indeed rises linearly along the torus from suction to discharge.

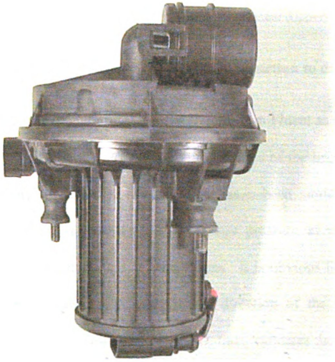

Figure 29: Electric air pump (Courtesy Pierburg)

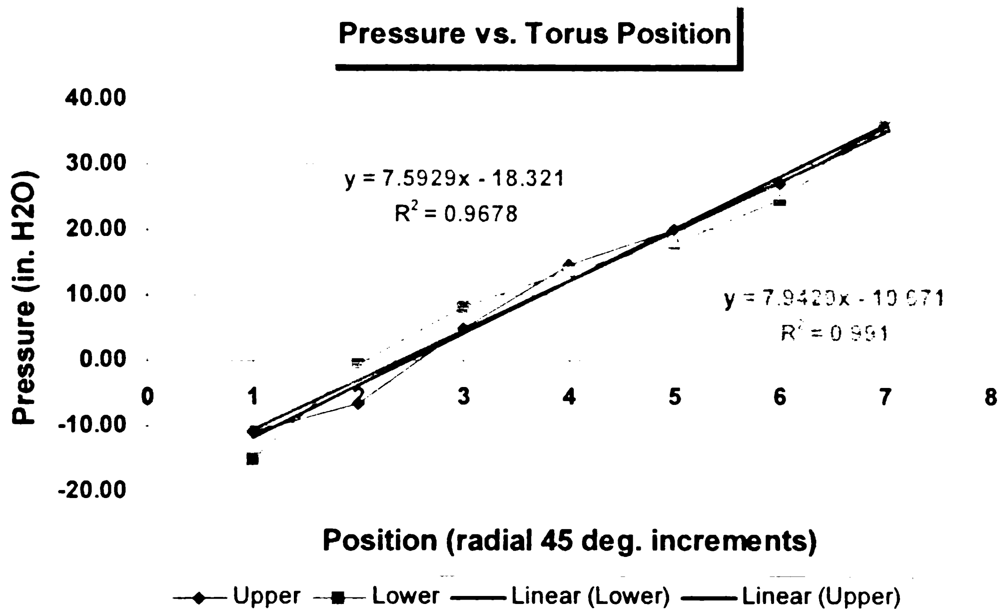

Figure 30: Pressure in the torus of the pump from suction to discharge

STAR CCM+ is a numerical simulation software different from Fluent as was mentioned; it is used to study the flow inside the pump. Both the air mass of the impeller and torus, which make up the entire air mass of the assembly, have been simulated at similar boundary conditions (0 Kpa, and 10 Kpa static gauge pressure at inlet and outlet respectively, and room temperature), and at 16,500 rpm. It is obvious that the pressure rises from suction (green) to discharge (red) in the direction of the rotation of the impeller, which is CCW as shown in Figure 31. CFD, thus, validates the theoretical and experimental results discussed earlier. Figure 32 is a close up view of the inlet area, where vacuum forms inside the pump. CFD and experimental tests were performed with different angles at inlet of pump, and the results show a 0.5 Kg/Hr of flow increase, and an overall performance increase at an angle of 60° from the horizontal.

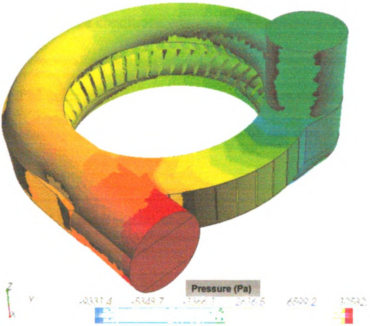

Figure 31: Contour plot of static pressure in the air mass of the air pump at 10 Kpa backpressure and 16,500 rpm

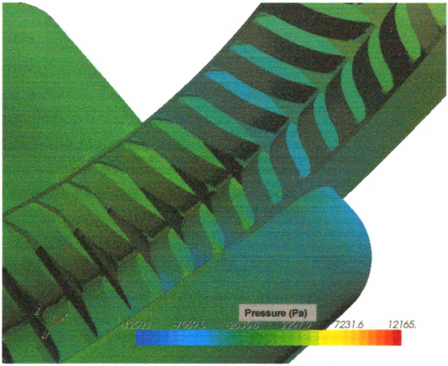

Figure 32: Contour plot of static pressure at the inlet region of the air pump at 10 Kpa backpressure and 16,500 rpm

The computational fluid dynamic simulations are performed on regenerative flow pumps with suction and discharge conditions corresponding to a pressure difference of 0 and 10 Kpa respectively at variable angular velocities. The data obtained for the outlet mass flow rate and RPM using CFD, is in good agreement with the experimental data obtained for the same boundary conditions, and a sample of the data for one RFP is shown in Figure 33.

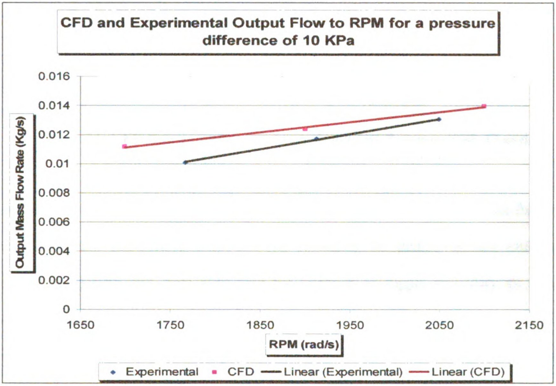

Figure 33: Flow rate Comparison of experimental and CFD data at various angular speeds

Using the performance prediction code, the number of blades on the rotor of the pump is another design parameter, which is shown to affect the flow and pump performance. To validate these findings numerical simulation tests were conducted on similar pumps with different numbers of blades namely 47, and 63 blades. Figure 34 shows a slight drop in flow using the 63 blades impeller; a finding, which was experimentally proven.

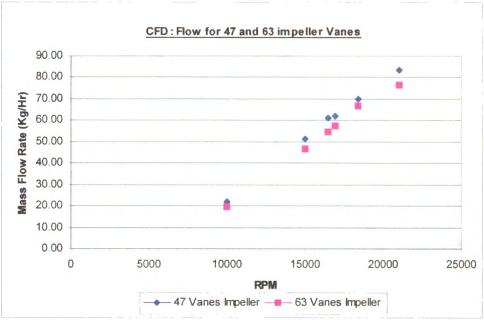

Figure 34: CFD flow comparison of two similar RFP pumps with 47 and 63 blades at 10 Kpa backpressure and various rpm values

Another test was conducted to measure the flow as a function of backpressure for both the filtered and non-filtered pumps. The secondary air pumps in this study are application specific, and were built with the intention to supply secondary air to the exhaust system in order to reduce emissions. Adding filters at the inlet is good practice to minimize damage done to the impeller blades and maximize the life cycle of the pump. Although, this addition come at a slight reduction of flow as illustrated in Figures 35 and 36. The test was carried out with two different designs. The pump impeller diameter and thickness, blade angle, and torus depth were modified and two different designs (A and B) with a reduction and an increase of these aforementioned parameter dimensions were tested, and the results are shown successively in Figures 36 and 37. Both pumps display similar trends, as the mass flow rate decreases with back pressure increase, accompanied with a linear increase in current draw, which is the same behavior predicted theoretically.

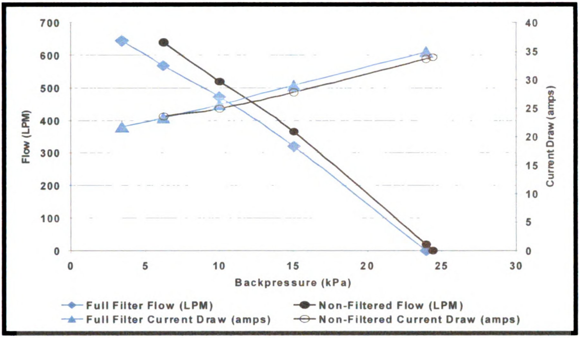

Figure 35: Mass flow rate and current draw as a function of backpressure for filtered and non-filtered pumps (Design A)

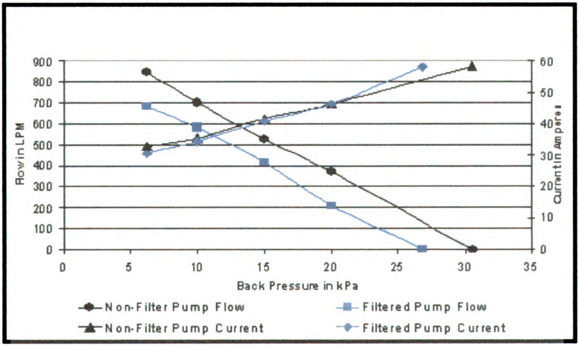

Figure 36: Mass flow rate and current draw as a function of backpressure for filtered and non-filtered pumps (Design B)

The closest competitor to the RFC based pumps are centrifugal pumps, which have been benchmarked against regenerative flow pumps for flow performance. The flows for both types of pumps were found to be comparable with slightly higher efficiency for the centrifugal pumps at higher flow rates and higher efficiency for regenerative pumps at lower mass flow rates. The big advantage, however, for the RFP, especially for this type of application of engine emission reduction, is its ability to reach fully operational steady state at a much faster rate than the centrifugal as is clearly shown in Figure 37. The pumps used for this experimental test are a scaled down version of the air pump model used in this study and centrifugal competitor pump production units. A run-down time comparison between the same pumps has been performed, and again the RFP proves to be at an advantage as shown in Figure 38.

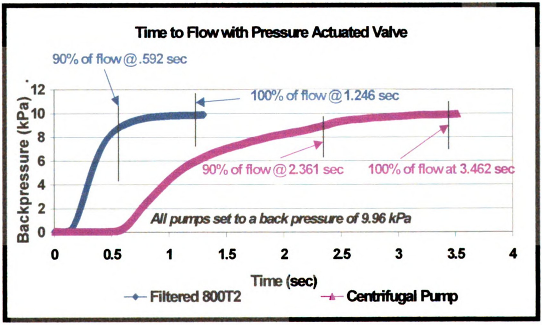

Figure 37: Time to flow comparison between an RFP and a centrifugal pump at 9.96 Kpa backpressure

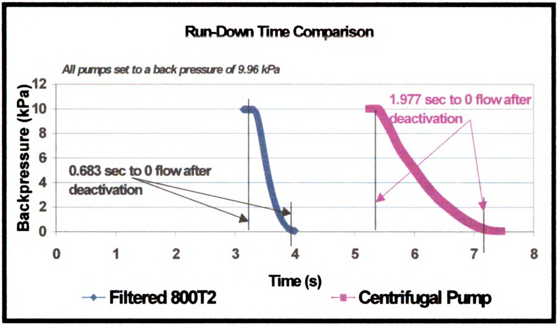

Figure 38: Run-down time comparison between an RFP and a centrifugal pump at 9.96 Kpa backpressure

Conclusion

The numerical simulations performed validated the experimental data obtained after running flow test on the prototypes. There was a good agreement between the two methods. This has been one of the objectives of this study as part of developing this new approach for the RFP performance enhancement. This is one part of a more comprehensive approach which, as was mentioned earlier, includes theoretical analysis, computational fluid dynamics simulations, and experimental testing. These results allow us to use a similar matrix for the input parameters when executing the performance prediction code and the numerical simulations.

CHAPTER 7

PERFORMANCE COMPARISON OF RADIAL, AEROFOIL, AND HYBRID BLADED GEOMETRY FOR RFC/RFP APPLICATION

7.1 Introduction

The effect of radial and non-radial blades on the performance of regenerative flow compressors and pumps is studied in this chapter. As was mentioned earlier in chapter 3, several researchers tried different design changes on both the torus and impeller of the regenerative flow compressors and pumps. The blade geometry, which was the most used in most of these research studies, was radial. Some of the authors who studied regenerative turbomachines with radial blades are Senoo [12, 39, 40, and 19], Gessner [34], Iverson [43], Shimosaka [42], and Grabow [44],

The mathematical modeling and the relative ease of manufacture of radial impeller prototypes made more popular amongst other blade geometries. The author noticed that, although the number of design parameters affecting the RFC performance is large, it could be narrowed down to several parameters such as the tip radius and stripper clearance as was discussed in chapter four. Such parameters, it was found, have the most effect on performance. The blade geometry is one of those parameters, which is predicted to have such an effect on efficiency, head and flow. For radial and aerofoil blade geometries, the blade geometry has a very noticeable effect on the performance of the compressors, as was verified in past studies. Sixsmith and Altmann [17] and Abdallah [22] studied the regenerative compressor with aerofoil blades. In the current chapter a third type of blading is introduced and is referred to here as Hybrid Blade which is really a combination of the radial and aerofoil blade. Various blade geometries for regenerative flow compressor impellers are shown in Figure 39.

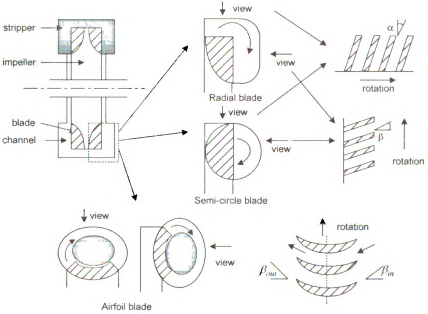

Figure 39: Various Blade Types for RFC/RFP

In this chapter overall comparisons of the three types of blade system for the RFC/RFP is carried out by considering, control volume modeling, governing equations and performance parameters, and comparison of the three blade systems in terms of the control volume modeling and flow governing equations.

7.2 Control Volume Modeling

The basic problem in the aerodynamic design of regenerative pumps/compressors is determining the maximum overall efficiency within certain limitations imposed by the type of application, and other considerations. There are few analytical models in literature, which explain the behavior of regenerative pumps and calculate their performance. Most of these models need extensive experimental support for performance prediction. For this reason, it is very important from an industrial point of view to find efficient theoretical models that can be used to predict the regenerative pump performance in more details.

7.2.1 Radial Blade

Radial blade geometries have been addressed in more than one occasion in different studies, including the one referred to in [22]. The following is a schematic showing a control volume of the radial blade geometry.

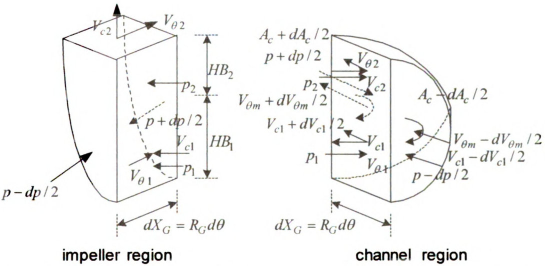

Figure 40: Control volumes representing section $d\theta$ of open channel and impeller for radial model [2]

7.2.2 Aerofoil Blade

Most designs of regenerative turbomachines in literature keep a reasonably basic geometrical configuration with simple vanes either machined or cast into the impeller. However, the addition of a core in the flow channel to direct the circulating flow together with the provision of airfoil blades was first shown by Sixsmith and Altmann [17]. They replaced the radial vanes by blades with an airfoil section. Blades were designed to transfer momentum to the fluid with a minimum of turbulence and friction. The annular channel had the core to assist in guiding the fluid such that it circulates through the blading while minimizing losses. The core also acted as a shroud to reduce losses due to formation of vortices at the tips of the blades. A typical RFC with airfoil blades is shown in Figure 41.

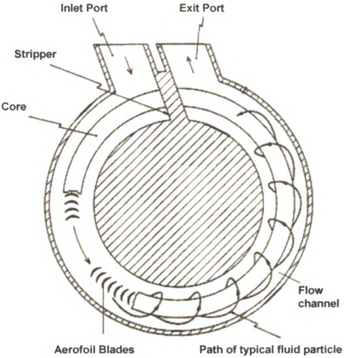

Figure 41: Regenerative Flow Pump with aerofoil blade geometry after [5]

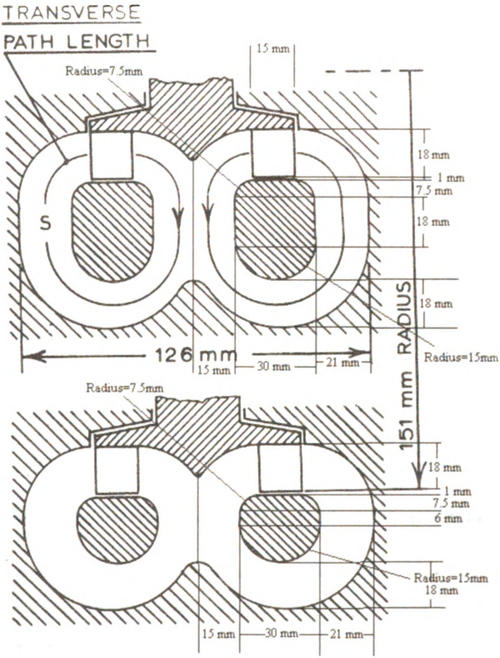

Figure 42: Regenerative compressor with airfoil blades (After Andrew [7])

7.2.3 Hybrid Blade

The hybrid blade geometry is a combination of both the radial and aerofoil blade geometries. It has not been given as much attention by researchers as the other blade geometries have, because of the introduction of the blade angle, which results in a more complex model. Manufacturing the impeller with such blading geometry poses more challenges as well, which makes even less attractive in the industrial field. A schematic of an impeller with hybrid blade geometry is shown in Figure 43.

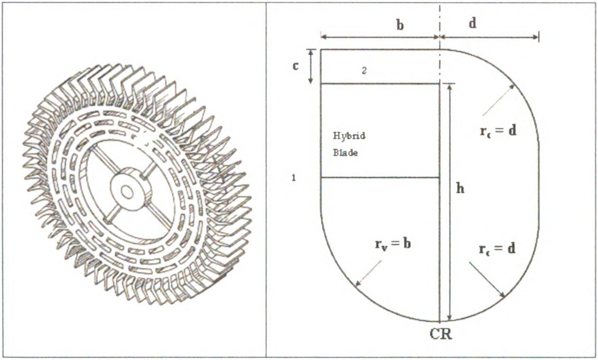

Figure 43: A hybrid impeller and hybrid impeller blade passage and channel

7.3 Governing Equations and Performance Parameters

To simplify the formulations and develop the analytical model, the following assumptions were made:

- Fluid is assumed incompressible locally within a control volume. The fluid is assumed incompressible throughout the pump operation and there is no variation in density from one control volume to the other.

- Steady flow without any leakages is assumed. Leakages are considered in a separate model to avoid complexity in mathematics. Thus leakages are assumed zero in the basic model.
- Characteristic flow is one-dimensional in which major direction is radial, tangential, and axial.
- There are no end effects of suction, discharge and stripper carryover. The inlet and exit losses are considered in a separate model.
- Tangential pressure gradient is independent of radius. Literature and experimental studies have confirmed that this assumption is quite valid.
- Although, tangential pressure gradient around the periphery is not perfectly linear, however for simplicity, assumption of linear pressure rise across the periphery is reasonable.
- Fluid shear is assumed negligible in the model.

The following equations are derived for the ideal model, which is restricted to the assumptions mentioned above and adapted to the influence of friction. This includes the Theoretical development of the equations for total head and efficiency.

7.3.1 Radial Blade

Analytical formulation is based on an arbitrary element of depth $dX_{Gi} = r_{Gi} d\theta$ in the peripheral direction of compressor as shown in Figure 45.

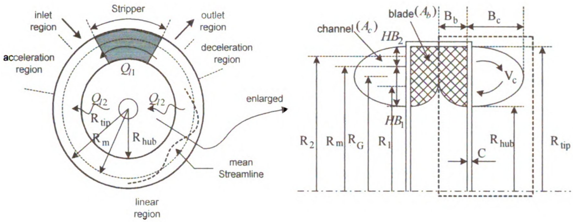

Figure 44: Schematic of blade and channel geometry for Radial model after [2]

Song [2], who also studied the radial blade geometry design assumed the tangential velocity as linear distribution in radial direction, the mean through-flow velocity $V_{\theta m}$ in the channel region can be related to the arithmetic mean of the tangential velocity entering and leaving the blade as follows.

$$Q = \int_{A_c} V_\theta \, dA_c = V_{\theta m} A_c \tag{48}$$

Where, $V_{\theta m} = (V_{\theta 1} + V_{\theta 2})/2$

After applying the angular momentum equation to channel region, the head rise is expressed in terms of the circulatory flow by using the continuity equation as:

$$dgH = dQ_c / Q_s (U_2 V_{\theta 2} - U_1 V_{\theta 1}) + V_{\theta m}^2 \, dA_c / A_c - dgH_L \tag{49}$$

In the right side of the above equation, the first term refers to head rise caused by momentum exchange of blade, the second term gives head rise caused by the deceleration of the mean tangential velocity and the last term gives head loss caused by friction and the contraction or expansion of the tangential velocity.

From equation (49), it is seen that the magnitude of the circulatory velocity changes head gradient. Because the difference of centrifugal force between blade and channel region is enlarged by increased channel area, the circulatory velocity increases rapidly, whereas the head gradient increase more than that in the constant channel area.

Where, $Q_s = \omega.R_G.A_c$ is the solid rotation in the channel and $R_G = 0.5(R_{tip} + R_{hub})$ is the centric radius of channel.

The expression for the overall fluid flow becomes:

$$Q / dQ_c V_c dV_c = (1 - Q / Q_s)(U_2 V_{\theta 2} - U_1 V_{\theta 1}) - gH_c \tag{50}$$

Where $gH_c = gH_{cb} + gH_{cc}$ is the sum of head loss related to the circulatory velocity.

The Angular momentum equation can be expressed as

$$d\hat{P}_{hyd} = \rho dQ_C \left(U_2 V_{\theta 2} - U_1 V_{\theta 1}\right) \tag{51}$$

and $$\hat{P}_{hyd} = \int_{X_G} d\hat{P}_{hyd} \tag{52}$$

$$\eta_{hyd} = \rho Q_r g H_{rise} / \hat{P}_{hyd} \tag{53}$$

7.3.2 Aerofoil Blade

A mean line representing the helical flow pattern inside a regenerative turbomachine by a streamline is used to simplify developing a mathematical model for the airfoil blade geometry. Because of helical flow pattern, this analysis is based on coordinates composed of radial R, circulatory ϕ and tangential direction θ as shown in Figure 44, which also shows the projected area and length of circulatory flow path in blade and channel region. The existence of a core, which is fixed to the channel helps to guide the fluid such that it circulates through the blade with a minimum loss.

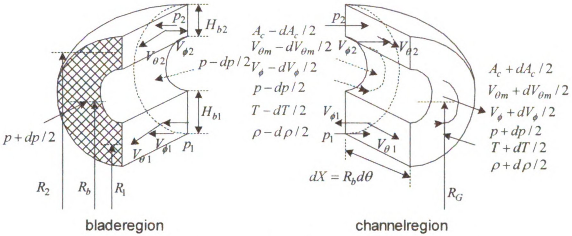

Figure 45: Arbitrary Control Volume for Aerofoil Model

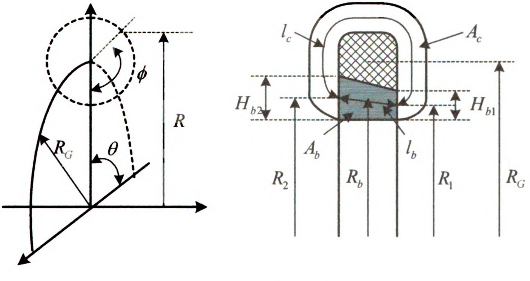

Figure 46: Coordinate and Meridional Geometry

In order to calculate pressure difference between incoming and outgoing flow in a control volume of blade region, Bernoulli equation along the streamline is applied and static pressure rise in the blade region is obtained as

$$\frac{p_2 - p_{1'}}{\rho} = (U_2 V_{\theta 2} - U_1 V_{\theta 1}) - V_{\theta m} .(V_{\theta 2} - V_{\theta 1}) - \frac{\Delta p_{\phi b}}{\rho} \tag{54}$$

Where, $\Delta p_{\phi b}$ is the pressure loss due to circulatory velocity through the blade region.

A slight difference in tangential location (θ) between the location where the mean streamline enters the blade row and the location where mean streamline exits the blade row $\theta_{1'}$ is denoted by $\Delta\theta_{2-1'}$ and is also shown in Figure 47.

Under the assumption that the relative tangential velocity within the blade is linearly distributed, equation 54 becomes

$$\frac{p_2 - p_1}{\rho} = (U_2 V_{\theta 2} - U_1 V_{\theta 1}) - V_{\theta m} .(V_{\theta 2} - V_{\theta 1}) - \frac{\Delta p_{\phi b}}{\rho} - \frac{\partial p}{\partial \theta} \Delta\theta_{2-1'} \tag{55}$$

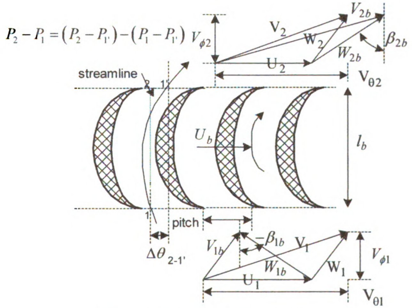

Figure 47: Velocity Triangles

The energy equation applied to blade control volume of Figure 46 yields

$$d\dot{P}_{hyd} = d\dot{m}_{\phi 2}h_{02} - d\dot{m}_{\phi 1}h_{01} + \left(h_0 + \frac{1}{2}U_b^2 - \frac{1}{2}V_{\theta m}^2 + \frac{dh_0}{2} - \frac{1}{2}d\left(\frac{1}{2}V_{\theta m}^2\right)\right)\left(\rho + \frac{d\rho}{2}\right)U_b A_b$$
$$-\left(h_0 + \frac{1}{2}U_b^2 - \frac{1}{2}V_{\theta m}^2 - \frac{dh_0}{2} + \frac{1}{2}d\left(\frac{1}{2}V_{\theta m}^2\right)\right)\left(\rho - \frac{d\rho}{2}\right)U_b A_b \tag{56}$$

$$\frac{d\dot{P}_{hyd}}{dX} = \rho V_\phi H_b\left(U_2 V_{\theta 2} - U_1 V_{\theta 1}\right) + \frac{d\rho}{dX}U_b^3 A_b$$

The hydraulic power and efficiency could be calculated using the following integrations

$$\dot{P}_{hyd} = \int_X d\,\dot{P}_{hyd} \tag{57}$$

$$\eta_{hyd} = \rho Q_r\left(\frac{gH_{rise}}{\dot{P}_{hyd}}\right) \tag{58}$$

7.3.3 Hybrid Blade

Regarding the RFC/RFP, it is strongly believed that quite a substantial additional pressure and gain in efficiency can be obtained from a good understanding of the exact flow mechanism, associated losses, and design changes to minimize the losses. An analytical model, which includes the different types of losses involved in RFC/RFP operation was developed and discussed in more detail in Chapter 5.

Analytical formulation is based on an arbitrary element of the control volume of differential angle dθ in the peripheral direction of compressor as shown in Figure 44. Considering these arbitrary small elements of one blade side and channel, equations of motion were derived. Dimensions of the impeller and flow channel are given symbolically in Figure 48 where points 1 and 2 denote the locations at which assumed streamline enters and leaves the impeller respectively.

The mechanism of operation of the RFC is described in terms of a circulatory flow (meridional flow), Q_c, superposed on a tangential (through flow), Q_T. The major quantities, which describe the operation of the ideal model, are the flow rate (Q) or capacity, total head (H), and hydraulic efficiency (h_{hyd}), for which equations are derived for the ideal model.

To simplify the model it is assumed that the flow has a helical path, and that all the flow leaves the impeller at the tip of the blades. Fluid is assumed incompressible locally within a control volume, and flow is steady without any leakages. Characteristic flow is one-dimensional in which major direction can have radial, tangential, and axial components. There are no end effects of suction, discharge and stripper carryover, and the tangential pressure gradient is independent of radius.

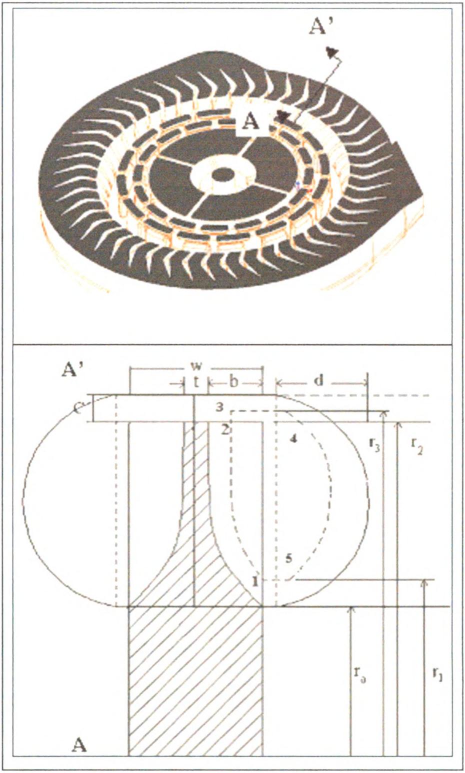

Figure 48: Schematic of cross sectional area of pump assembly and section AA' of one blade passage

The expression obtained for the tangential through flow along the linear section of the channel is equation 59.

$$Q=\sigma r_2 U_2\left[b\ln(r_3/r_4)+d\ln(r_3/r_1)+\frac{A_2}{r_3}+\frac{A_4}{r_1}\right]-\left(\frac{\partial p}{\partial\theta}\frac{d\theta}{d\dot{m}}\right)\left[\begin{array}{l}\frac{(r_3+r_2)A_1}{2}\left(\frac{b}{2}+\frac{A_2}{r_3}+\frac{A_4}{r_1}\right)- \\ \frac{(r_3+r_1)A_3}{2}\left(\frac{A_4}{r_1}-\frac{d}{2}\right)+\frac{A_2^2}{2}+\frac{A_2A_4r_3}{r_1}+ \\ \frac{A_4^2}{2}-\left(\frac{b^2r_2^2}{2}\ln(\frac{r_3}{r_2})\right)+ \\ \ln(\frac{r_3}{r_1})\left(dr_3A_2+\frac{d^2r_3^2}{2}+\frac{d(r_3+r_2)}{2}\right)\end{array}\right] \tag{59}$$

This expression for the flow could be simplified without much loss in accuracy to get:

$$Q=S_1\sigma r_2 U_2-S_2\left(\frac{\partial p}{\partial\theta}\frac{d\theta}{d\dot{m}_c}\right) \tag{60}$$

Where

$$S_1=\left[b\ln(r_3/r_4)+d\ln(r_3/r_1)+\frac{A_2}{r_3}+\frac{A_4}{r_1}\right]$$

$$S_2=\left[\begin{array}{l}\frac{(r_3+r_2)A_1}{2}\left(\frac{b}{2}+\frac{A_2}{r_3}+\frac{A_4}{r_1}\right)- \\ \frac{(r_3+r_1)A_3}{2}\left(\frac{A_4}{r_1}-\frac{d}{2}\right)+\frac{A_2^2}{2}+\frac{A_2A_4r_3}{r_1}+ \\ \frac{A_4^2}{2}-\left(\frac{b^2r_2^2}{2}\ln(\frac{r_3}{r_2})\right)+ \\ \ln(\frac{r_3}{r_1})\left(dr_3A_2+\frac{d^2r_3^2}{2}+\frac{d(r_3+r_2)}{2}\right)\end{array}\right]$$

For the RFC, the total head and the developed volume rate of flow of the fluid pumped is of interest. This includes the pressure rise and the mass flow rate. The head and enthalpy change in return is related to the net mechanical energy added to the fluid in the pump. Considering the radial or circulatory flow Q_c for half of the pump, and the change over the angle θ of the working section of the pump, the theoretical total head rise developed by the ideal model is defined as:

$$\Delta H = \frac{Q_C \cdot (\sigma . r_2 U_2 - \alpha . r_1 U_1)}{A . r_g} \tag{61}$$

Because of the loss of mechanical energy by mechanisms such as wall friction and turbulence, the total head, as determined by measurement, is less than the head computed using equation 61 above. Considering the inlet and discharge losses, the general expression for head rise will be:

$$\Delta H = H_r + \Delta H_f \tag{62}$$

Where H_T is the actual total head developed by the pump, and H_f is the term representing the head loss. This loss term includes the inlet and outlet discharge losses, irreversibilities through the stripper associated with the impeller, and head drop through the working section. Assuming that the radial and tangential losses are proportional to the square of the flow rate, and assuming a constant of proportionality $k_t \approx$2E+3 [44],

$$\Delta H_f = k_t Q^2 \tag{63}$$

In the impeller or casing passages, the flow is accompanied by frictional losses. All losses convert mechanical energy into thermal energy. Wall friction effects, for instance, by viscous forces and by turbulence generation cause direct dissipation of energy.

Secondary flow losses occur in regions of flow separation, where circulation is maintained by external flow and in curved flow passages where it is maintained by centrifugal effects.

Although, the practical mechanical energy losses discussed above are accounted for by considering the hydraulic performance parameter as determined by testing is the overall pump efficiency, the efficiency.

$$\eta_{hyd} = \frac{Q}{Q_s} \tag{64}$$

Where Q_s is the flow the pump would deliver if solid body rotation with respect to rotor velocities were obtained and it is expressed as:

$$Q_s = 2A.\omega.r_g \tag{65}$$

Including loss terms, the efficiency is expressed as

$$\eta_{hyd} = \frac{Q}{Q_s}\left(\frac{H_T}{H_T + H_f}\right) \tag{66}$$

7.4 Comparison of the three blade systems

Flow Modeling

The overall RFC geometry is very comparable for all three blade configurations. The regenerative flow compressor or pump usually has an impeller, a torus, a suction and a discharge, and of course electric motor and other accessories. In this chapter the concern is mainly the impeller, and specifically, the impeller blade geometry. The impeller has vanes machined into either one side or both sides at its periphery, which due to their rotation produce a series of helical flow pattern, returning the fluid repeatedly through the vanes for additional energy as it passes through an open annular channel (torus). The fluid does not discharge freely from the tips of the blades but circulates back to blades many times before leaving the impeller, thus the term regenerative, which the name of the turbomachine implies. The helical flow motion has a gradual increase of air pressure in the tangential direction.

In all three models one blade passage and the corresponding channel area were chosen for modeling. Because of the circulatory flow inside the blade passage and the channel, understanding the flow behavior in these two regions is important.

The continuity, momentum, and energy equations are applied to each control volume of the blade geometry and steady flow is assumed to the circulatory flow. The meridional pressure drop in the open channel is then obtained. The circulatory flow is one of the main components, which changes in these equations of motion between the different blade geometries. For instance in the case of the radial blade applying the angular momentum equation to the impeller control volume we get

$$dT = \rho dQ_c \left(r_2 \sigma U_2 - r_1 \alpha U_1\right) + r_G A_b \frac{dp}{d\theta} d\theta \qquad (67)$$

Where Q_c is the circulatory flow, and which in the case of the hybrid takes on the following form

$$dQ_C = br_2 V_{C2} \cos(\gamma) d\theta = yr_1 V_{C1} d\theta \qquad (68)$$

Where γ is the angle of curvature of the blade, which is null for the radial blade.

Chapters 4 and 5 have more detailed derivations of these equations.

In the case of aerofoil blade geometry the continuity and momentum equations were slightly different because of the blade curvature, although a similar control volume is used. For continuity,

For continuity, ignoring flow leakages, it was assumed that the total mass flow rate in tangential direction remains constant and could be calculated by adding mass flow rates through channel and blade cross sectional areas. Moreover, total mass flow rate is also equal to the summation of mass flow rate entering the compressor through the inlet port and mass flow rate carried over by the blades through the stripper to the flow channel, which is referred as carryover mass flow rate denoted by $\dot{m}_s$. Continuity is then expressed in the following form

$$\dot{m}_c + \dot{m}_b = \rho V_{\theta m} A_c + \rho U_b A_b = \dot{m} + \dot{m}_s \tag{69}$$

Where, the mean tangential velocity$(V_{\theta m})$ in the channel region is calculated as the average of tangential velocities at R_1 and R_2.

For momentum, applying the angular momentum equation to channel region in tangential direction, we get

$$\left[\left(\dot{m}_c + \frac{d\dot{m}_c}{2}\right)\left(V_{\theta m} + \frac{dV_{\theta m}}{2}\right) - \left(\dot{m}_c - \frac{d\dot{m}_c}{2}\right)\left(V_{\theta m} - \frac{dV_{\theta m}}{2}\right)\right] r_G + d\dot{m}_\phi \left(r_1 V_{\theta 1} - r_2 V_{\theta 2}\right)$$
$$= r_G \left(p - \frac{dp}{2}\right)\left(A_c - \frac{dA_c}{2}\right) - r_G \left(p + \frac{dp}{2}\right)\left(A_c + \frac{dA_c}{2}\right) + r_G\, p\, dA_c - \int_{A_\tau} r\tau\, dA_\tau \tag{70}$$

Applying momentum equation in the circulatory direction and simplifying, we get

$$\left(\dot m_\phi + \frac{d\dot m_\phi}{2}\right)\left(V_\phi + \frac{dV_\phi}{2}\right) - \left(\dot m_\phi - \frac{d\dot m_\phi}{2}\right)\left(V_\phi - \frac{dV_\phi}{2}\right) + \cancel{d\dot m_{\phi 1}V_\phi} - \cancel{d\dot m_{\phi 2}V_\phi} \\ = \left(p_2 - p_1\right) dA_\phi - \Delta p_{\phi c} dA_\phi \tag{71}$$

After some manipulations, we get the governing equation for circulatory velocity which can be expressed as a highly non-linear differential equation

$$\frac{dV_\phi^2}{dX} = 2\frac{V_\phi H_b}{V_{\theta m} A_c}\left(\frac{p_2 - p_1}{\rho} - \frac{\Delta p_{\phi c}}{\rho}\right) + 2\left(\frac{V_\phi}{V_{\theta m}}\right)^2 \frac{1}{\rho}\frac{d\rho}{dX}\frac{A_b}{A_c} U_b V_{\theta m} \tag{72}$$

In the blade region, the angular momentum equation can be given as,

$$d\dot P_{hyd} = \omega dT \tag{73}$$

$$d\dot P_{hyd} = d\dot m_c\left(U_2 V_{\theta 2} - U_1 V_{\theta 1}\right) + \left(\rho + \frac{d\rho}{2}\right) U_b A_b U_b^2 - \left(\rho - \frac{d\rho}{2}\right) U_b A_b U_b^2 \\ + \left(p + \frac{dp}{2}\right) U_b A_b - \left(p - \frac{dp}{2}\right) U_b A_b \tag{74}$$

Simplifying we get,

$$d\dot P_{hyd} = d\dot m_c\left(U_2 V_{\theta 2} - U_1 V_{\theta 1}\right) + d\rho U_b A_b U_b^2 + \cancel{dpU_b A_b} \tag{75}$$

Dividing by dX and ignoring the last term in above equation because of negligible pressure rise in the blade region, we get

$$\frac{d\dot P_{hyd}}{dX} = \rho V_\phi H_b \left(U_2 V_{\theta 2} - U_1 V_{\theta 1}\right) + \frac{d\rho}{dX} U_b^3 A_b \tag{76}$$

If last term is ignored in R.H.S. of the above equation, first term refers to power consumed in momentum exchange of blade and the second term represents increment in power caused by increment in density.

Thus, it can be seen that the same approach has been taken to choose the control volumes for the three different blade geometries, and also similar method is used to derive the equations of motion of the fluid in both the blade passage and channel (torus). Based on these analytical models derived, performance prediction codes were written to predict the performance characteristics of the different impeller blade geometries, which is the subject of the following segment.

Performance prediction code

Based on proposed analytical formulation for incompressible flow and loss models, a performance prediction code is developed for all three blade geometries, and numerical results are obtained for different geometrical configurations of the RFC, namely radial, aerofoil, and hybrid, which are compared to each other. The non-linear ordinary differential equations of the flow inside the impeller and channel were solved for arbitrary control volumes as was mentioned earlier. The performance prediction code takes geometric and inlet flow conditions as input and predicts head rise, efficiency, and other properties. These predictions allow us top determine the design parameters, which have the most impact on performance.

The performance prediction code was designed with the following assumptions, which are based on experimental data for similar devices.

Steady and compressible flow of fluid which is considered as an ideal gas $p = \rho R_{gas} T$. Helical flow can be described by a mean streamline with tangential velocity V_θ and circulatory velocity V_ϕ or V_c at any position. Circulatory velocity, density, and temperature are considered to vary only along the tangential direction i.e. $(V_\phi$ or V_c $,\rho,T,p) = f(R,\phi,\theta)$. All pressure losses can be categorized into losses related to circulatory and tangential velocity.

Some of the numerical values for different parameters and coefficients, which are held constant, are:

Slip factor SIGMA: $\sigma = 0.85$. This coefficient, which is the ratio of the fluid velocity to the blade velocity at the periphery, might be higher (0.85-0.95). This coefficient accounts for discrepancy caused by secondary flow, and it is a function of only the design of the rotor, and its value is constant in all cases. Slip angle GAMA: $\gamma = 20^{o}$, which is the actual value for T3's vane internal angle, although values ranging from 20^{o} to 45^{o} have been also used.

The coefficient (α) is the ratio of the fluid velocity to the blade velocity at the base of the blade. It is dependent at the point of operation on the head capacity curve because of the variation in the velocity profile as operating conditions are changed. It is the ratio of the tangential velocity of the fluid to the velocity of the blade at the vane base. It spans from shut off (maximum head -- Q=0), where it is negative ($\alpha<0$) to maximum capacity (Qmax), where it becomes positive ($\alpha>0$). Capacity increases with α, and it is positive at high flows (observed experimentally). This is responsible for the directional change of the tangential velocity at the blade entrance. α = [-1.0 -- 1.0] (α=0, is where the optimum efficiency point lies, as was proven experimentally). Tangential loss coefficient: k = 2,000, and Vane spacing = 0.411 average.

Using this code with the input parameters similar to the ones mentioned above, several design parameters were determined as having the most effect on performance. Blade angle, height, width, and blade angle which form the blade geometry are few of these parameters. Blade angle of 0 for the radial and angles of 20 to 45 for the radial blade have been tested, along with the aerofoil blade.

Blade geometry efficiency

Blade number does affect the blade geometry considering there are a finite number of blades in each RFC impeller. The number of blades is optimized as was described in chapter 4. It is worth mentioning that Iverson [43] reported the experimental effect of blade number on regenerative pump performance. He tested impellers with 31, 36 and 39 blades and found that the pump head and efficiency were increased with an increase in the number of blades within the tested range.

During the course of this thesis the author was able to confirm Iverson's findings; however, the author also found out that there is an upper limit on the number of blades without losing the optimum efficiency. The optimum number of blades for the greatest head at a given flow rate we found to be in the range between 47 and 63 blades. Burton [15] reported that the pump performance could be improved by using a non-radial blade. The shut-off head coefficient obtained by using a blade angle was nearly twice of that obtained by using the straight blade. Yamazaki [45, 46, and 47] studied non-radial blades and Grabow [41] and Hollenberg [33] studied the semi-circular blade shapes. Grabow reported theoretical and experimental effects of the blade angle for both radial and semi-circular blades. He tested the pump in both cases with different blade angles and found from the theoretical research that the optimum shut off head was reached for the blade angle in the range of 40^{o}-55^{o}, whereas experimental study resulted in optimal blade angle in the range of 40^{o}-45^{o}. Abdallah [22] found from the theoretical study of the blade angle effect on the shut-off head that optimum range of aerofoil blade angle is 55^{o}-61^{o}. In this study however the author found out that the optimum blade angle is in the range 28^{o}-40^{o} for hybrid blade geometry.

For all three blade geometries it was found that the efficiency is generally low at lower flow rates and it increases as the flow rate through the pump increases. This is characteristic of RFP, which suggests that in order to get good efficiency; the pump should be operating at a higher flow rate. The reason for low efficiency at low flow rate, the author believes, is that the circulatory power is more at low flow rates due to increased number of circulations at low flow rates, which is a cause of increasing circulatory head loss. When flow rate increases through the pump, there are fewer circulations which mean better efficiency. The radial blade design however has shown to be slightly more flow. There is always a tradeoff between efficiency and head in the case of regenerative flow compressors and pumps.

Performance characteristics comparison

Sixsmith compared the performance of a radial blading RFC/RFP with an aerofoil blading. Input parameters were chosen to estimate these performance parameters. Some of these parameters are a mass flow rate of 45Kg/Hr, a rotational speed of 4,000 rpm, and a pressure differential of 2Kpa, and a pressure ratio of 1.17. Sixsmith showed that the efficiency rose from 45% for the radial blade to 58% for the aerofoil blade, the head coefficient also increased by a factor of 2.8 and the flow coefficient increased by a factor of 3.14. These gains are obtained with the specific speed reduced by a factor of 0.9. The authors in this thesis took this study further and compared the performance of the hybrid blade geometry to with both the aerofoil and radial blades. The authors showed that the efficiency rose from 45% to 54% for the hybrid blade and was comparable to that of the aerofoil blade. The hybrid blade geometry showed an improvement over both the radial and aerofoil blade geometries for both the head and flow, although the specific speed is reduced for the hybrid blade geometry. These results are summarized below and show the superiority of the hybrid blade geometry.

Performance	Formula	Wilson, Santalo, & Oelrich	Sixsmith & Altmann	Elkacimi & Engeda
Efficiency	$\frac{\dot{m} RT \ln(P_2/P_1)}{ShaftPower}$	45%	58%	54%
Specific Speed	$\frac{nQ^{1/2}}{(gH)^{3/4}}$	0.244	0.220	0.167
Head Coefficient	$\frac{gH}{U^2}$	1.5	4.2	4.4
Flow Coefficient	$\frac{Q}{D^2U}$	0.014	0.044	0.064

Performance characteristics comparison for radial, aerofoil, and hybrid blade geometries

CHAPTER 8

COMPREHENSIVE DESIGN METHODOLOGY

8.1 Comprehensive Design Methodology for RFC/RFP

The approach taken in this thesis to study the performance of regenerative flow compressors and pumps is comprehensive in that it included theoretical analysis, numerical simulation, and experimental work. The focus of this thesis was mainly on the 'hybrid' blade geometry of RFC/RFP, although the radial and airfoil blade geometries were also studied. A mathematical model for the RFC was developed and equations representing the performance characteristics were deduced. These characteristics are mainly the head rise, hydraulic efficiency, and current draw. An expression for the overall flow through the compressor / pump was also derived based on the geometrical configuration of the pump and compressor. Because of the operational similarity of the regenerative flow pumps and compressors, the same mathematical model was used to develop a performance prediction code for both. Using known design and input parameters, this one-dimensional code is able to predict the performance of the pump/compressor in terms of the performance characteristics mentioned earlier. Several design parameters were identified analytically, and their number was narrowed down by the author through a performance study, and the parameters having the most influence on the pump performance were used for design changes. The mathematical model was designed to be very flexible and could be applied to different impeller and torus geometries of regenerative flow compressors.

Once the performance is rated through the use of the performance prediction program and the design parameters having the largest effect on the performance are determined, then recommendations for design changes on the pump or compressor could be made. Any design tool, such as Unigraphics or Pro-e which was used in this study, could then be employed to make the design changes on the actual model. Air-mass on which performance simulation is to be performance, is then extracted from the solid model. Different computational fluid dynamics software packages are used to simulate the flow behavior inside the pump and predict the pump/compressor performance. In this study both FLUENT and STAR CCM+ were used for such purpose. Because of the complexity of the models for the RFC, special care is taken to make sure that the 3-dimensional simulations are fully ran without making any assumptions as to the symmetry of the model. The regenerative flow pumps and compressors are not symmetrical due to the configuration of the suction and discharge, and also because the channel around the impeller (torus) does not have constant cross sectional area.

Most of the studies performance in the past on RFC/RFP, where some of the CFD work has been done studied the flow performance in one blade passage in an impeller. Then the results were extrapolated to predict the flow behavior in the rest of the impeller. Of course this approach has its drawbacks, and limitations, but has been and is still acceptable considering the limitations of the software programs and machine computational power currently available. The author in this thesis took the challenging task of simulating the entire air-mass of the pump and compressor three-dimensionally, and used the actual operational and input parameter values to perform these full-scale numerical simulations. The advantage this method has over the others, in spite of its complexity, is that it allows for a better understanding of the flow behavior inside the pump or compressor, and a complete visualization of the effect of the different input parameters on performance.

Prototypes were built for the pumps and compressors with the design changes recommended based on the performance prediction code. These prototypes were tested and the results were found to validate the theoretical and numerical simulation results. To build the prototypes stereolithography was the method used for fabrication, although other fabrication techniques could be used as well.

A systematic approach to improve compressor and pump efficiency outlined and described in detail in this thesis, and could be applied to any regenerative flow compressor or pump. Instead of relying on the engineering intuition to recommend design changes to improve the performance of regenerative flow compressors and pumps as it has been done so far in most of the industry related to emission reduction using RFC/RFP, this methodical approach combining theoretical analysis, numerical simulation, and computational fluid dynamics is very useful in efficient. In this approach the purpose of building prototypes and testing them was to validate the CFD and theoretical predictions. But the objective of this approach is to actually reduce or eliminate the use of prototypes to reduce the cost of product development. One of the intentions of the author was to streamline the research and development processes at BorgWarner and develop a system, which would allow the engineers to predict the performance of flow compressors and pumps, recommend design changes based on performance and sensitivity analysis of the performance prediction code and computational fluid dynamics simulations respectively.

8.2 Future Applications/Recommendations

As was discussed earlier in this study, the choice of peripheral compressors or RFC's over other types of compressors, such as centrifugal, rotary lobe, diaphragm, or reciprocating piston, all of which can be used in applications requiring high delivery head at low flow rates is based on many factors. First of all, the positive displacement types are inferior due to problems associated with lubrication, sealing, wear, and diaphragm life, which contribute to high initial and maintenance costs. For emission reduction and control applications, which is the target of this study, centrifugal compressors are the most likely competitors. While it is true that centrifugal compressors are inherently more efficient than regenerative flow compressors, performance-wise, this is only accurate under many conditions. The RFC is a low specific speed machine, and within its normal range of specific speeds, its efficiency compares favorably with that of centrifugal compressors. Moreover, one of the most important structural advantages of RFC types is that it does not have any complex flow passages and no vaning is required. Centrifugal compressors also require higher rotating speeds and/or larger number of stages, and because of surge characteristics, stage matching becomes more critical and off-design operation more restricted with the centrifugal compressors than with the peripherals.

These advantages of RFC over their counterparts, lead us to believe that number and type of applications for this type of compressors is wide and diverse. The applications will go beyond the current automotive functions and expand into the aerospace, medical, and even the MEMS (Micro-Electro-Mechanical Systems) to name a few. More research needs to be done on different models of RFC exploring a variety of blade geometries and design parameters. Applications in the MEMS area need more theoretical studies, since some of the Newtonian mechanics will not hold for small (microns in magnitude) regenerative flow pumps and compressors.

The analysis presented in this dissertation was focused on performance prediction and improvement through theoretical modeling, computational fluid dynamics, and sensitivity analysis. These tools which take in the geometry data and predict the performance are developed in this study. The next step is to extend such tools to design mode and allow the researcher or engineer to specify the desired operating point and immediately size the compressor dimensions including those for the impeller, channel, inlet and outlet ports, and stripper design. Today there is a need to develop several design criteria in terms of non-dimensional parameters, which would lead to development of a generic design code. This code would take the desired operating point and size the compressor dimensions. Considering the scarcity of literature on the subject for RFC/RFP and the lack of efficient tools to size up and improve the designs of these turbomachines, the tools developed in this study will serve to get the industry closer to a more streamlined tool, which could facilitate product research and development of these pumps and compressors.

APPENDICES

APPENDICES

APPENDIX A:

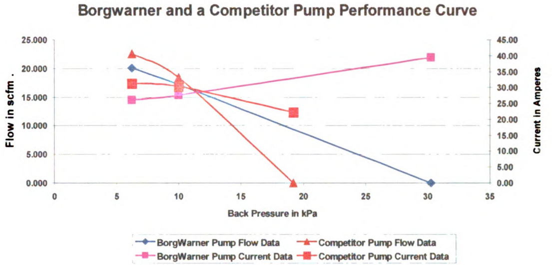

Figure 49: Research model and a Competitor RFP Performance Curve

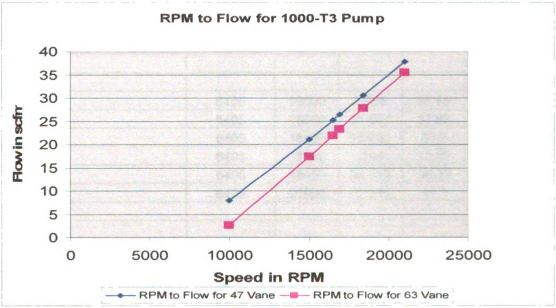

Figure 50: RFP research models (prototypes) Flow Curves

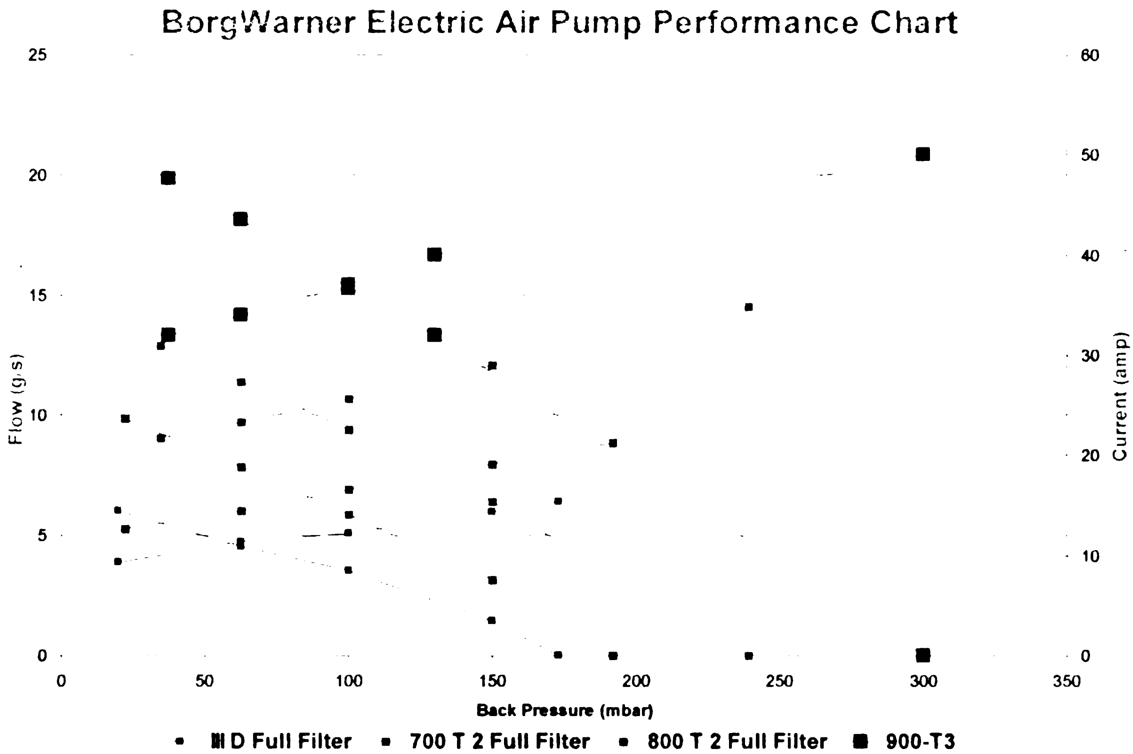

Figure 51: Research model Secondary Air Pump (RFP) Performance Curves

Impeller	Pump Number	RPM	Flow	Current	Voltage
			Scfm	Amperes	Volts
47 Vane	6405	10000	7.938	25.85	7.75
47 Vane	6405	15000	21.057	31.63	11.22
47 Vane	6405	16500	25.231	33.7	12.25
47 Vane	6405	16950	26.4	33.99	12.61
47 Vane	6405	18400	30.519	36.33	13.7
47 Vane	6405	21000	37.745	41.1	15.68
63 Vane SLA	6405	10000	2.561	26.3	7.66
63 Vane SLA	6405	15000	17.358	31.22	11.05
63 Vane SLA	6405	16500	21.88	33.75	12.04
63 Vane SLA	6405	16950	23.338	32.4	12.3
63 Vane SLA	6405	18400	27.803	34.21	13.36
63 Vane SLA	6405	21000	35.508	38.78	15.42

Research model Performance Data for Two Impellers with Different Blade Numbers

Sr. No.	Pump Number	Supplier #	Flow	Current	Speed	DH Pressure	DH Current	DH Speed
			Scfm	Amperes	rpm	" of H2O	Amperes	rpm
	Acceptance Criteria							
47 Vane Standard Impeller at 13.5 Volts & 40"								
	6405		29.665	35.75	18113	111.4	59.08	14479
	6346		29.716	36.34	18375	116.4	62.33	14857
63 Vane SLA Impeller at 13.5 Volts & 40"								
	6405		28.577	34.84	18582	N/A	N/A	N/A
	6346		28.426	35.28	18628	N/A	N/A	N/A
47 Vane Standard Impeller at 13.5 Volts & 25"								
	6405		36.048	32.78	18957			
	6346		35.147	32.43	18841			
63 Vane SLA Impeller at 13.5 Volts & 25"								
	6405		34.858	31.62	19160			
	6346		34.425	31.74	19109			
47 Vane Standard Impeller at 11.0 Volts & 40"								
	6405		20.688	32.45	15057	93.1	50.34	12850
	6346		20.11	32.19	15002	88.2	49.49	12593
63 Vane SLA Impeller at 11.0 Volts & 40"								
	6405		17.913	31.08	15173	72	43.1	13886
	6346		16.779	32.22	14941	72	43.51	13421
47 Vane Standard Impeller at 11.0 Volts & 25"								
	6405		26.857	28.2	15630			
	6346		26.23	26.84	15572			
63 Vane SLA Impeller at 11.0 Volts & 25"								
	6405		25.716	26.3	15853			
	6346		24.965	26.38	15618			

Research model Performance Data for Two Impellers with Different Blade Numbers both standard and SLA

APPENDIX A:

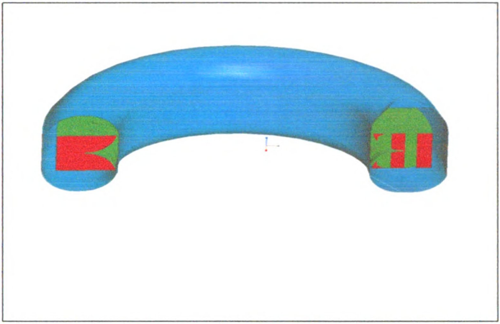

Figure 52: Cross-Sectional Area of Torus and Peripheral part of Impeller for Hybrid RFP

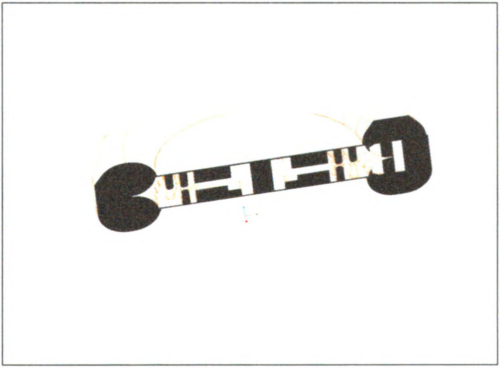

Figure 53: Cross-Sectional Area of Torus and Impeller for Hybrid RFP

Figure 54: Cross-Sectional Area of Torus and Peripheral part of Impeller for Hybrid RFP

REFERENCES

REFERENCES

[1] Principles of Turbomachinery. R.K. Turton. E. & F. N. Spon Ltd, 1984

[2] Roth,M.,Peikert,R.: Flow visualization for turbomachinery design, Proc. IEEE Visualization '96, (1996) pp.381-384.

[3] Toward Excellence in Turbomachinery Computational Fluid Dynamics: A Hybrid Structured-Unstructured Reynolds-Averaged Navier-Stokes Solver. Hong Yang, Dirk Nuernberger, Hans-Peter Kersken. ASME J. Turbomachinery APRIL 2006, Vol. 128. pp 390-402.

[4] http://www.bath.ac.uk/~en1lagc/Engineering/aeroengines/axial.htm

[5] Iverson H. W., "Performance of the Periphery Pump", Trans. of ASME, Jan. 1955, pp 19-28.

[6] Brennen, C. E., "Hydrodynamics of Pumps", NREC 1994

[7] Whitehead D. S., Harrison S., and Rose M. G. "A Regenerative Compressor," Cambridge University, Cued/A- Turbo/Tr 114, 1982.

[8] Hollenberg J. W., "An investigation of the efficiency of regenerative blowers and pumps", PhD thesis, Stevens institute of technology, 1978.

[9] Crewdson E., "Water-Ring Self-Priming Pumps", Proceeding of the Inst. of Mech. Engr., Vol. 170, No.13, 1956, pp 407-417.

[10] Iverson H. W. Performance of the Periphery Pump. Trans. of ASME, Jan. 1955, pp. 19-28.

[11] Balje O. E., "Drag-Turbine Performance", Trans. of ASME, August. 1957, pp 1291-1304.

[12] Senoo Y., "Theoretical Research on Friction Pump", Reports of Research Institute for Fluid Engineering, Kyusku University, Vol.5, No.1, 1948, pp 23-28.

[13] Jakubowski M., Kovitz A.A, and Raynor S., "Ideal Fluid Flow in an Enclosure of Toroidal Geometry, Int. J. Non Linear Mechanics, Vol. 6 (1971) pp 101-115 pergamon press.

[14] Wilson W. A., Santalo M.A., and Oelrich J. A. A Theory of the Fluid-dynamic Mechanism of Regenerative Pumps. Trans. of ASME, Nov. 1955, pp. 1303-1316.

[15] Burton J. D., "The prediction and improvement of regenerative turbomachine performance", The British hydromechanics research association, 9th member conference, Cranfield, September 1967.

[16] Iverson H. W. Performance of the Periphery Pump. Trans. of ASME, Jan. 1955, pp. 19-28.

[17] Sixsmith H. and Altmann H. "A Regenerative Compressor," J. of Engineering for Industry, Aug. 1977, pp 637-647.

[18] Mason S. C. Influence of Internal Geometry upon Regenerative Pump Performance. B.S. thesis, MIT, May 1957.

[19] Senoo Y., "Influences of the Suction Nozzle on the Characteristic of a Peripheral Pump and an Effective Method of their Removal", Reports of Research Institute for Applied Mechanics, Kyusku University, Vol.3, No.11, August 1954, pp 129-142.

[20] Shimosaka M., Yamazaki S., "Research on the characteristics of Regenerative Pump", Bulletin of JSME, Vol. 3, No. 10, 1960, pp. 185-190.

[21] Senoo Y., "Researches on the Peripheral Pump", Reports of Research Institute for Applied Mechanics, Kyusku University, Vol.3, No.10, July1954, pp 53-113.

[22] Abdalla H.M.M., "A Theoretical and Experimental Investigation of the Regenerative Pump with Airfoil Blades, PhD thesis, September 1981, Applied Mechanics Branch, Royal Military College of Science.

[23] Gessner R.L., "Multistage, Gas-Bearing, Helium Compressor Development", Advances in Cryogenic Engineering, 1966, pp 631-639.

[24] Meakhail, T., Seung O. P., Dae Sung Lee, and Mikhail S. A study of circulating flow in regenerative pump. Proceedings of the KSAS 1st International Session. 2003, Gyeongju, pp. 19–26.

[25] A.J. Glassman. Turbine Design and Application, vol.1, NASA SP-290. 1972

[26] D.G.Wilson, T. Korakianiti. The Design of high-Efficiency Turbomachinery and gas Turbines. 1998.

[27] Badami, M. Theoretical and experimental analysis of traditional and new periphery pumps. SAE Technical Paper Series, no. 971074, 1997, pp. 45–55.

[28] Song J. W., Engeda A., and Chung M. K. A modified theory for the flow mechanism in a regenerative flow pump. Proc. Instn Mech. Engrs Part A: J. Power and Energy, 2003, 217, 311–321.

[29] Rasmussen, B. D. and Jakobsen, A. (2002). Review of compressor models and perfor-mance characterizing variables. In Soedel, W., editor, 2002 International Compressor Engineering Conference at Purdue, volume 1, pages 515–522, West Lafayette, Indiana, USA. Ray W. Herrick Laboratores.

[30] K. Ueno, and R. E. Bye, VAIREX Corporation K. S. Hunter, University of Colorado, Compressor Efficiency Definitions, May 12th, 2003.

[31] Idelchick, I. E. Handbook of Hydraulic Resistance, 3rd edition, 1993 (Begell House, New York).

[32] Engineering Edge. http://www.engineersedge.com/

[33] Hollenberg J. G., "Hydrogen Pipeline Transmission", Stevens Institute of Technology, Hoboken, New Jersey 07030.

[34] Gessner R.L., "Multistage, Gas-Bearing, Helium Compressor Development", Advances in Cryogenic Engineering, 1966, pp 631-639.

[35] Abdalla H.M.M., "A Theoretical and Experimental Investigation of the Regenerative Pump with Airfoil Blades, PhD thesis, September 1981, Applied Mechanics Branch, Royal Military College of Science.

[36] Andrew D.N., "The Calculation of Flow in Regenerative Turbomachines by a Streamline Curvature Method", Proc. Instn. Mech. Engrs., Part A: J. of Power and Energy, Vol. 204, 1990. pp 121-129.

[37] Hong Yang, Dirk Nuernberger, Hans-Peter Kersken. Toward Excellence in Turbomachinery Computational Fluid Dynamics: A Hybrid Structured-Unstructured Reynolds-Averaged Navier-Stokes Solver. ASME J. Turbomachinery APRIL 2006, Vol. 128. pp 390-402.

[38] Sheng, C., 2004, "Full Annulus Simulation of a High-Speed Centrifugal compressor Using an Unstructured RANS Flow Solver," ASME Paper No. GT2004-53657.

[39] Senoo Y., "A Comparison of Regenerative Pump Theories Supported by New Performance data", Trans. of ASME, Vol. 78, July. 1956, pp 1091-1102.

[40] Senoo Y., "Researches on the Peripheral Pump", Reports of Research Institute for Applied Mechanics, Kyusku University, Vol.3, No.10, July1954, pp 53-113.

[41] Grabow G., "Influence of the Number of Vanes and Vane Angle on the Suction Behaviour of Regenerative Pumps", Proceedings Conference on Fluid Machinery (5^{th}) Budapest. Hungry, September 15-20, 1975, Vol. 1, pp 351-364.

[42] Shimosaka M., "Research on the characteristics of Regenerative Pump", Bulletin of JSME, Vol. 3, No. 10, 1960, pp. 191-199.

[43] Iversen H.W., "Performance of the Periphery Pump", Trans. of ASME, Jan. 1955, pp 19-28.

[44] Wilson W. A., Santalo M.A., and Oelrich J. A. A Theory of the Fluid-dynamic Mechanism of Regenerative Pumps. Trans. of ASME, Nov. 1955, pp. 1303-1316.

[45] Yamazaki S., Tomita Y., "Researches on the Performance of the Regenerative Pump with Non-radial Vanes", Bulletin of JSME, Vol. 14, No. 77, 1971, pp. 1178-1186.

[46] Yamazaki S., Tomita Y., "Researches on the Performance of the Regenerative Pump with Non-radial Vanes", Bulletin of JSME, Vol. 15, No. 81, 1972, pp. 337-343.

[47] Yamazaki S., Tomita Y., "Researches on the Performance of the Regenerative Pump with Non-radial Vanes", Bulletin of JSME, Vol. 17, No. 106, 1974, pp. 459-466.

[48] Sixsmith H., "The design of a regenerative compressor for the "ISABELLE" refrigerator" Brookhaven national laboratory, Technical Note No. 31, January, 1977.

[49] Ohba H., Nakashima Y., Shiramoto K., Shiramoto K., "A Study on Performance and Internal Flow Pattern of A vertex Pump", Bulletin of JSME, Vol. 21 No.162, 1978 , pp 1741-179.

[50] Ohba H., Nakashima Y., "Studies on the Internal Flow and Performance of the Vortex Pump and Application to Slurry Transporting", Memoirs of the Faculty of Engineering, Kumamoto University, Vol. 29, No. 1, March 1984, pp 1-31.

[51] Oelrich J. A., "Development of an Analysis of a Regenerative Pump", M. I. T. Ph. D Thesis, 1953.

[52] Aoki M., "Studies on the Vortex Pump (2nd Report)", Bulletin of JSME, Vol. 26, No. 213, March 1983, pp 384-398.

[53] Jae Wook Song, Doctoral Thesis, Investigation on the Performance Analysis of Regenerative Turbomachines, Korea Advanced Institute of Science and Technology, 2004.

[54] Muhammad Mukarrum Raheel, "A Theoretical, Experimental, and CFD Analysis of Regenerative Flow Compressors and Pumps for Microturbine and Automotive Fuel Applications, Doctoral Dissertation, Michigan State University, 2003.

[55] Moffat R., "Is there a small Compressor in your Future?", Hydraulics & Pneumatics, pp160-258.